

An information-theoretic branch-and-prune algorithm for discrete phase optimization of RIS in massive MIMO

I. Zakir Ahmed, *Member, IEEE*, Hamid R. Sadjadpour, *Senior Member, IEEE*, and Shahram Yousefi, *Senior Member, IEEE*

Abstract—In this paper, we consider passive RIS-assisted multi-user communication between wireless nodes to improve the blocked line-of-sight (LOS) link performance. The wireless nodes are assumed to be equipped with Massive Multiple-Input Multiple-Output antennas, hybrid precoder, combiner, and low-resolution analog-to-digital converters (ADCs). We first derive the expression for the Cramer-Rao lower bound (CRLB) of the Mean Squared Error (MSE) of the received and combined signal at the intended receiver under interference. By appropriate design of the hybrid precoder, combiner, and RIS phase settings, it can be shown that the MSE achieves the CRLB. We further show that minimizing the MSE w.r.t. the phase settings of the RIS is equivalent to maximizing the throughput and energy efficiency of the system. We then propose a novel Information-Directed Branch-and-Prune (IDBP) algorithm to derive the phase settings of the RIS. We, for the first time in the literature, use an information-theoretic measure to decide on the pruning rules in a tree-search algorithm to arrive at the RIS phase-setting solution, which is vastly different compared to the traditional branch-and-bound algorithm that uses bounds of the cost function to define the pruning rules. In addition, we provide the theoretical guarantees of the near-optimality of the RIS phase-setting solution thus obtained using the Asymptotic Equipartition property. This also ensures near-optimal throughput and MSE performance.

Index Terms—Cramer-Rao lower bound, Chow-Lee algorithm, Kullback-Leibler divergence, asymptotic equipartition property, typical set, Markov decision process.

I. INTRODUCTION

The Reconfigurable Intelligent Surfaces (RIS) are known to mitigate the harsh effects of wireless channels such as obstruction, shadowing, fading, and other complex scenarios encountered between the transmitter and receiver of interest. This is achieved by efficient beamforming and interference management by the RIS. The RIS comprises an array of large number of reflecting elements, each of which can be controlled to change the amplitude, delay (phase shift), and polarization of the incident signal from the transmitter. In the case of passive RIS structures, only the phase of the incident signal is changed, and the RIS consumes no power in such a situation. In one of the typical architectures, the desired phase shift to be induced upon the incident signal can be achieved by controlling the bias voltage to the positive-intrinsic-negative

(PIN) diode associated with each of the RIS elements [1].

The vehicular communication frameworks, namely Vehicle to Everything (V2X) based on the IEEE 802.11p Wireless Local Area Network (WLAN) and the Cellular-V2X (C-V2X) defined by the 3GPP and 5G Automotive Association (5GAA) aim to achieve the goals of the Intelligent Transportation Systems (ITS) [2], [3]. The objectives of the ITS include collision avoidance, ease road congestion, accident information, pedestrian safety, emergency vehicle approach warning, and parking assistance, to name a few. With the adoption of massive Multiple-Input Multiple-Output (MaMIMO), millimeter-wave (mmWave), and Terahertz (THz) communications in the next generations of wireless communication, it is natural that the vehicular communication nodes will encompass them in the future. A millimeter MaMIMO framework for C-V2X is proposed and studied in [4]. Vehicular wireless links are prone to significant challenges due to the highly dynamic nature of the channels due to large buildings, continuous traffic, and changing landscapes. The integration of the RIS technology to vehicular communication is being studied in the literature and has shown promising results. They are shown to maximize the sum V2X link capacity while guaranteeing the minimum SINR of the vehicle-to-vehicle links [5]–[7].

RIS is one of the key enablers for the sixth-generation (6G) mobile communication networks. This is particularly useful for problems of coverage extension in mmWave and THz communication systems due to the unfavorable free-space omnidirectional path loss in these frequency bands [8], [9]. In addition to enhancing the wireless link's performance between the transmitter and receiver, the RIS has found applications in providing physical layer security. Advanced signal processing techniques are used to manipulate the wireless channel using RIS to guarantee the security of the communication content in an information-theoretic sense. Essentially the RIS ascertains physical-layer security by configuring the RIS elements in such a fashion to add the wireless signals constructively to the legitimate receiver but destructively to a potential eavesdropper [10]. A few other examples of the applications of RIS include enhancing the link performance of the cell-edge users who suffer high signal attenuation from the base station (BS), co-channel interference from near BSs [11], [12], Interference management to support low-power transmission to enhance individual data links in device-to-device networks [13], In non-orthogonal multiple-access (NOMA) systems, RIS could be considered to increase the number of served users and

I. Zakir Ahmed and Hamid R. Sadjadpour are with the Department of Electrical and Computer Engineering, University of California at Santa Cruz, Santa Cruz, CA 95064 USA. Shahram Yousefi is with the Department of Electrical and Computer Engineering, Queens University, Kingston, ON K7L 3N6, Canada.

enhance the rate of communication, which constitutes the major requirement to be accomplished in these systems [12], [14], [15]. Improve the link performance between the unmanned aerial vehicle (UAV) network and the ground users for UAV trajectory optimization and improve overall system performance, including energy efficiency [16].

The fundamental problem in all of the above applications is configuring the RIS phase-shift setting to achieve a specific goal. Finding an optimal RIS configuration for a set of K discrete phase shifts with M element array has an exponential time complexity $O(K^M)$. In addition, the objective function is often non-convex in the decision parameters (RIS phase shift settings). Identifying the optimal RIS phase shift is a non-convex NP-Hard combinatorial optimization problem.

The proposed algorithm benefits several similar problems related to the wireless backhaul link in the vehicular network or the roadside unit layer, vehicle-to-everything framework, and cellular systems, to name a few.

A. Related works

Previously, a branch-and-bound (BnB) algorithm was used to solve an optimization problem involving RIS phase shifts to maximize the spectral efficiency (SE) [17]. A block-coordinated descent algorithm to maximize the achievable up-link rate with multiple single-antenna users and multi-antenna base stations was proposed in [18]. There, resolution-adaptive analog-to-digital converters (ADCs) operating at millimeter-wave (mmWave) frequencies were assisted by a passive RIS. A trace-maximization-based optimization framework was presented in [19] to study the effect of the link capacity in a point-to-point MIMO link that considers two RIS architectures. A trellis-based joint optimization of the beamformer and the RIS discrete phase shifts to minimize the mean squared error (MSE) of the received symbols was proposed in [20]. In [21], a RIS-assisted architecture is proposed to maximize channel power gains between two users in a NOMA framework. A branch-and-bound (BnB) algorithm is used to solve an optimization problem involving RIS phase shifts to maximize the spectral efficiency (SE) in [17]. The solution obtained is achieved by linear approximation of the objective function involving the phase shifts of the RIS. Also, the SE maximization is accomplished by relaxing it to a convex problem. RIS-assisted optimal beamforming for a Multiple-Input Single-Output (MISO) communication system is proposed in [22]. An optimal global solution using BnB is claimed in it. However, the results obtained are not compared with the exhaustive search technique. In addition, the bounds for the BnB algorithm are obtained using convex approximations. The authors in [23] propose a low-complexity algorithm using alternating optimization (AO) to jointly optimize transmit-beamforming and RIS phase shift settings to minimize the transmit power from the multi-antenna access point (AP) to multiple single-antenna users. A RIS-aided point-to-point multi-data-stream MIMO is studied in [24]. An AO-based algorithm to jointly optimize the RIS phase shifts and precoder is investigated in it to minimize the symbol rate error. However, the combiner design is not considered in this work.

Also, the optimality guarantees of the proposed AO algorithm are not investigated. In [25], a RIS-aided MIMO simultaneous wireless information and power transfer (SWIPT) for Internet-of-Things (IoT) networks are investigated. A BnB algorithm is proposed to maximize the minimum signal-to-interference-plus-noise ratio (SINR) among all information decoders (IDs) while maintaining the minimum total harvested energy at all energy receivers (ERs). In it, the authors relax the quadratic assignment problem to a linear integer problem and use the BnB method to obtain the solution. A joint multi-UAV trajectory/communication optimization problem in a network with RISs on uneven terrain is proposed in [26]. An effective path-planning algorithm for this optimization problem is proposed. Although the paper deems that the issue of RIS control (either phase-shift or amplitude) is beyond its scope, a mathematically rigorous proof of its asymptotic optimality is given. However, the problem considered is a continuous optimization problem, and the computational complexity of the approach is not discussed in it. An asymptotic analysis for RIS assisted communication between multi-antenna users for mmWave MaMIMO is studied in [27]. The problem of minimizing the transmit power subject to the rate constraint is also analyzed for the scenario without direct paths in the pure LOS propagation.

All the earlier works in literature make convex approximations of the objective function under consideration and solve the same using various well-established algorithms, for example, Branch-and-Bound (BnB). However, to the best of our knowledge, none of the earlier works show theoretical guarantees for either optimality or near-optimality, considering the original non-convex problem.

B. Our contribution

In this paper, we consider a RIS-assisted multi-user MaMIMO communication system under interference. The contributions of this paper are as follows: (i) We first derive the expression for the Cramer-Rao lower bound (CRLB) of the MSE of the received and combined signal as a function of the phase settings of the RIS for a given hybrid precoder, combiner, and ADC bits,

(ii) we show that minimizing the MSE by adjusting the RIS phase shifts also ensures maximization of throughput and energy efficiency,

(iii) we show that the MSE achieves the CRLB with the appropriate design of the hybrid precoders, and combiners,

(iv) we present a novel Information-Directed Branch-and-Prune (IDBP) algorithm, in which, we, to the best of our knowledge, for the first time in the literature use an information-theoretic measure to decide on the pruning rules in a tree-search algorithm to arrive at the RIS phase-setting solution, which is vastly different compared to the traditional branch-and-bound algorithm that uses bounds of the cost function to define the pruning rules.

(v) we establish theoretical guarantees for near-optimality, and substantiate the claims by comparing the solutions obtained with the exhaustive search method for a smaller value of M .

(vi) We compare the performance and the time complexity

of the proposed algorithm with the state-of-the-art trace-maximization-based approach for MIMO transceiver structure proposed in [19], and the AO algorithm proposed in [24], both for larger M .

C. Notations

The column vectors are represented as boldface small letters and matrices as boldface uppercase letters. The primary diagonal of a matrix is denoted as $\text{diag}(\cdot)$, and all expectations $E[\cdot]$ are over the random variable \mathbf{n} , which is an AWGN vector. The multivariate normal distribution with mean $\boldsymbol{\mu}$ and covariance $\boldsymbol{\varphi}$ is denoted as $\mathcal{N}(\boldsymbol{\mu}, \boldsymbol{\varphi})$ and $\mathcal{CN}(\mathbf{0}, \boldsymbol{\varphi})$ denotes a multivariate circularly-symmetric Gaussian distribution. The trace of a matrix \mathbf{A} is shown as $\text{tr}(\mathbf{A})$ and \mathbf{I}_N represents a $N \times N$ identity matrix. The frobenius norm of matrix \mathbf{A} is indicated as $\|\mathbf{A}\|_F$. The superscripts T and H denote transpose and Hermitian transpose, respectively. The terms \mathbb{R} , and \mathbb{C} indicate the space of real, and complex numbers, respectively.

D. Paper content

The rest of this paper is organized as follows. Section II describes the system model and parameters. In Section III, we describe the hybrid precoder and combiner design. We discuss the RIS phase shift optimization and derive the optimization framework in Section IV. Section IV also details the design to fine-tune the digital precoders and combiners. We describe the theoretical framework of the proposed IDBP algorithm in Section V, including the optimality analysis. The proposed IDBP algorithm is detailed in Section VI. The computational complexity analysis is described in Section VII, followed by simulation results in Sections VIII, and conclusions in Section IX respectively. Supporting Theorems and their proofs are presented in the Appendices.

II. SIGNAL MODEL

We consider a RIS equipped with M passive reflecting elements each of which can be set to K discrete phase-shift values to aid the millimeter-wave (mmWave) Massive Multiple-Input Multiple-Output (MaMIMO) communication between two roadside units (RSU) in a vehicular wireless backhaul network, typically called the RSU-to-RSU wireless link. In addition, we consider the RSUs to be equipped with hybrid precoders, hybrid combiners, and low-resolution ADCs. The communication is assumed to have a blocked line-of-sight (LoS) signal to the intended RSU receiver. An example use-case scenarios is illustrated using Fig.1 [4]. This proposed signal model can be extended to other use-case scenario like V2X, cellular wireless backhaul network nodes without loss of generality.

The signal model of such a communication system is shown in Fig.2. Here, we denote \mathbf{F}_D and \mathbf{F}_A to be the digital and analog precoders, respectively. Similarly, we represent \mathbf{W}_D^H and \mathbf{W}_A^H to be the digital and analog combiners, respectively. The vector \mathbf{x} is an $N \times 1$ transmitted signal vector whose average power is unity. Let N_{rt} and N_{rs} denote the number of RF Chains at the transmitter and receiver, respectively.

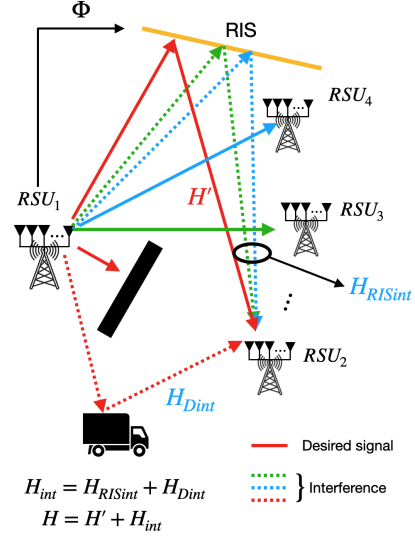


Fig. 1: An example of an RSU layer employing a RIS for enhancing the performance of a blocked LOS link under Interference.

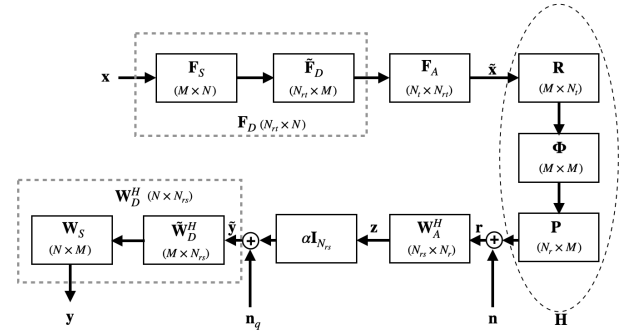


Fig. 2: System model with RIS-assisted channel with interference.

Also, N_t and N_r represent the number of transmit and receive antennas, respectively. The effective channel \mathbf{H} which is a $N_r \times N_t$ matrix at the intended receiver will be a combination of the RIS reflected signal from the transmitter and the interference of the signal from the same transmitter intended for the other multi-antenna users. That is

$$\mathbf{H} = \mathbf{H}' + \mathbf{H}_{int}, \quad (1)$$

where the channel \mathbf{H}' represents the blocked LOS channel between TX and RX assisted by the RIS in the absence of interference, and can be expressed as $\mathbf{H}' = \mathbf{Q}\boldsymbol{\Phi}\mathbf{G}$. The term $\mathbf{G} \in \mathbb{C}^{M \times N_t}$ is the transmitter-to-RIS (TX-RIS) channel, $\mathbf{Q} \in \mathbb{C}^{N_r \times M}$ being the RIS-to-receiver (RIS-RX) channel [19]. The action of the M element RIS is represented as $\boldsymbol{\Phi} = \text{diag}(e^{j\phi_1}, e^{j\phi_2}, \dots, e^{j\phi_M})$. Here $\phi_n \in \Phi$, where Φ is a finite set phase angles with cardinality K .

The interference channel \mathbf{H}_{int} represents the combination of the RIS reflected signals from the transmitter to the other users but arriving at the intended receiver \mathbf{H}_{RISint} , and the non-LOS reflected from the transmitter to the receiver not going

through the RIS \mathbf{H}_{Dint} (See Fig. 1). Formally

$$\mathbf{H}_{int} = \mathbf{H}_{RISint} + \mathbf{H}_{Dint} = \sum_{i=1}^{\beta} \mathbf{Q}_i \Phi \mathbf{G}_i + \mathbf{H}_{Dint}, \quad (2)$$

where the components $\{\mathbf{G}_i\}_{i=1}^{\beta}$ represent the transmitter-to-RIS of the interferers, similarly $\{\mathbf{Q}_i\}_{i=1}^{\beta}$ are the RIS-to-receiver channels of the interferers, with β indicating the total number of interferers. Hence the effective channel between the TX and the RX considering the interferers can be written as

$$\mathbf{H} = \mathbf{H}' + \mathbf{H}_{int} = \mathbf{Q}\Phi\mathbf{G} + \sum_{i=1}^{\beta} \mathbf{Q}_i \Phi \mathbf{G}_i + \mathbf{H}_{Dint}. \quad (3)$$

Inspired by the channel model adopted in [19], [27], we express the RIS-assisted channel with interference given in (3) as a traditional mmWave MIMO channel comprising of γ paths (here $\gamma = \beta + 2$, see (3))

$$\mathbf{H} = \mathbf{A}_r \mathbf{D} \mathbf{A}_t^H, \quad (4)$$

where \mathbf{D} is a $\gamma \times \gamma$ diagonal matrix comprising of the complex gains $\{\alpha_i\}_{i=1}^{\gamma}$, the matrices \mathbf{A}_r and \mathbf{A}_t correspond to the collection of the steering vectors $\mathbf{a}_r(\phi_r)$, $\mathbf{a}_t(\theta_t)$ with ϕ_r^i and θ_t^i indicating the angles of arrival and departures respectively. That is

$$\begin{aligned} \mathbf{A}_r &= [\mathbf{a}_r(\phi_r^1), \mathbf{a}_r(\phi_r^2), \dots, \mathbf{a}_r(\phi_r^\gamma)], \\ \mathbf{A}_t &= [\mathbf{a}_t(\theta_t^1), \mathbf{a}_t(\theta_t^2), \dots, \mathbf{a}_t(\theta_t^\gamma)]. \end{aligned} \quad (5)$$

Now, when we choose the number of TX antennas N_t and RX antennas N_r to be very large, the Singular Value Decomposition (SVD) of the matrix \mathbf{H} in (4) can be shown as [27]–[29]

$$\mathbf{H} = \mathbf{U}\Sigma\mathbf{V}^H = [\mathbf{A}_r | \mathbf{A}_r^\perp] \Sigma [\tilde{\mathbf{A}}_t | \tilde{\mathbf{A}}_t^\perp]^H, \quad (6)$$

where Σ is a diagonal matrix comprising of the singular values on its diagonal

$$[\Sigma]_{ii} = \begin{cases} |\alpha_i|, & \text{for } 1 \leq i \leq \gamma \\ 0, & \text{for } i > \gamma, \end{cases} \quad (7)$$

and the matrix

$$\tilde{\mathbf{A}}_t = [e^{j\zeta_1} \mathbf{a}_t(\theta_t^1), e^{j\zeta_2} \mathbf{a}_t(\theta_t^2), \dots, e^{j\zeta_\gamma} \mathbf{a}_t(\theta_t^\gamma)], \quad (8)$$

where ζ_i is the phase component of the complex gain α_i . Taking into account the action of the RIS phase shifts Φ , we can rewrite (6) as

$$\begin{aligned} \mathbf{H} &= \mathbf{U}\Sigma\mathbf{V}^H = [\mathbf{A}_r | \mathbf{A}_r^\perp] \Sigma [\tilde{\mathbf{A}}_t | \tilde{\mathbf{A}}_t^\perp]^H, \\ &= \mathbf{U}\Sigma\Phi\mathbf{R} = \mathbf{P}\Phi\mathbf{R}, \end{aligned} \quad (9)$$

where $\mathbf{R} = \text{diag}(e^{j\zeta_1}, e^{j\zeta_2}, \dots, e^{j\zeta_{(\beta+1)}}, \dots) \mathbf{V}^H$, and $\mathbf{P} = \mathbf{U}\Sigma$. It is to be noted that \mathbf{P} and \mathbf{R} are not unitary matrices anymore. Hence we can visualize the effective channel \mathbf{H} as

$$\mathbf{H} = \mathbf{P}\Phi\mathbf{R}. \quad (10)$$

$\mathbf{R} \in \mathbb{C}^{M \times N_t}$ is the effective transmitter-to-RIS (TX-RIS) channel, $\mathbf{P} \in \mathbb{C}^{N_r \times M}$ the RIS-to-receiver (RIS-RX) channel, both considering the interference.

In this work, we focus on minimizing the mean squared

error (MSE) performance of the communication link by optimizing the phase shifts. The transmitted signal $\tilde{\mathbf{x}}$ and the received signal \mathbf{r} are represented as

$$\tilde{\mathbf{x}} = \mathbf{F}_A \mathbf{F}_D \mathbf{x}, \quad \mathbf{r} = \mathbf{H} \tilde{\mathbf{x}} + \mathbf{n}. \quad (11)$$

Here, \mathbf{n} is an $N_r \times 1$ noise vector of independent and identically distributed (i.i.d) complex Gaussian random variables such that $\mathbf{n} \sim \mathcal{CN}(\mathbf{0}, \sigma_n^2 \mathbf{I}_{N_r})$. The received symbol vector \mathbf{r} is analog-combined with \mathbf{W}_A^H to get $\mathbf{z} = \mathbf{W}_A^H \mathbf{r}$ and later digitized using a low-resolution ADCs to produce $\tilde{\mathbf{y}} = \mathbf{Q}_b(\mathbf{z}) = \alpha \mathbf{I}_{N_{rs}} \mathbf{z} + \mathbf{n}_q$. The quantizer $\mathbf{Q}_b(\mathbf{z})$ is modeled as an Additive Quantization Noise Model (AQNM), where $\alpha = 1 - \frac{\pi\sqrt{3}}{2} 2^{-2b}$, and b is the bit resolution of the ADCs employed across all the RF paths [30], [31] in the receiver. The vector \mathbf{n}_q is the additive quantization noise which is uncorrelated with \mathbf{z} and has a Gaussian distribution: $\mathbf{n}_q \sim \mathcal{CN}(\mathbf{0}, \mathbf{D}_q^2)$ [30], [31]. This signal is later combined using the digital combiner \mathbf{W}_D^H to produce the output signal $\mathbf{y} = \mathbf{W}_D^H \tilde{\mathbf{y}}$.

The relationship between the transmitted signal vector \mathbf{x} and the received symbol vector \mathbf{y} at the receiver is given by

$$\mathbf{y} = \alpha \mathbf{W}_D^H \mathbf{W}_A^H \mathbf{P} \Phi \mathbf{R} \mathbf{F}_A \mathbf{F}_D \mathbf{x} + \alpha \mathbf{W}_D^H \mathbf{W}_A^H \mathbf{n} + \mathbf{W}_D^H \mathbf{n}_q, \quad (12)$$

where the dimensions of the hybrid precoder and combiner are as follows: $\mathbf{F}_D \in \mathbb{C}^{N_{rt} \times N}$, $\mathbf{F}_A \in \mathbb{C}^{N_t \times N_{rt}}$, $\mathbf{W}_A^H \in \mathbb{C}^{N_{rs} \times N_r}$, and $\mathbf{W}_D^H \in \mathbb{C}^{N \times N_{rs}}$.

The precoders \mathbf{F}_D and \mathbf{F}_A , and combiners \mathbf{W}_D^H and \mathbf{W}_A^H are designed for a given channel realization \mathbf{H} . We assume that the perfect channel state information \mathbf{P} and \mathbf{R} are known both to the transmitter and the receiver, and the topic of channel estimation is outside the scope of this paper. We further assume that the number of RF paths N_{rs} on the receiver is the same as the number of parallel data streams N . The analysis is easy to extend and similar for the case $N_{rs} \neq N$.

Mean squared error performance:

It can be shown that the expression for the MSE δ of the received, quantized, and combined signal \mathbf{y} using (12) as

$$\delta \triangleq \text{tr}(\mathbf{M}(\mathbf{x})), \quad (13)$$

where $\mathbf{M}(\mathbf{x})$ is the MSE matrix that can be written as

$$\begin{aligned} \mathbf{M}(\mathbf{x}) &= (E[(\mathbf{y} - \mathbf{x})(\mathbf{y} - \mathbf{x})^H]), \\ &= p(\mathbf{K} - \mathbf{I}_N)(\mathbf{K} - \mathbf{I}_N)^H + \alpha^2 \sigma_n^2 \mathbf{W}\mathbf{W}^H + \mathbf{W}_D^H \mathbf{D}_q^2 \mathbf{W}_D. \end{aligned} \quad (14)$$

Here $\mathbf{K} = \alpha \mathbf{W}_D^H \mathbf{W}_A^H \mathbf{P} \Phi \mathbf{R} \mathbf{F}_A \mathbf{F}_D$, $E[\mathbf{x}\mathbf{x}^H] = p\mathbf{I}_N$, $\mathbf{W} = \mathbf{W}_D^H \mathbf{W}_A^H$, $E[\mathbf{n}\mathbf{n}^H] = \sigma_n^2 \mathbf{I}_{N_r}$, $E[\mathbf{n}_q \mathbf{n}_q^H] = \mathbf{D}_q^2$, $\mathbf{D}_q^2 = \alpha(1 - \alpha) \text{diag}[\mathbf{W}_A^H \mathbf{H} (\mathbf{W}_A^H \mathbf{H})^H + \mathbf{I}_{N_{rs}}]$, $E[\mathbf{n}\mathbf{n}_q^H] = 0$, and p is the average power of the symbol \mathbf{x} .

The design of the precoder, combiner, and the RIS phase-shift settings to minimize the MSE δ for a given b -bit ADC

can be posed as a multi-dimensional optimization problem

$$(\mathbf{F}_A^{opt}, \mathbf{F}_D^{opt}, \mathbf{W}_A^{Hopt}, \mathbf{W}_D^{Hopt}, \Phi^{opt}) = \underset{\mathbf{F}_A, \mathbf{F}_D, \mathbf{W}_A^H, \mathbf{W}_D^H, \Phi}{\operatorname{argmin}} \delta. \quad (15)$$

If the precoders, combiners, and the RIS phase settings are chosen such that $\mathbf{K} = \mathbf{I}_N$, then the MSE matrix $\mathbf{M}(\mathbf{x})$ can be written as

$$\mathbf{M}(\mathbf{x}) = \alpha^2 \sigma_n^2 \mathbf{W} \mathbf{W}^H + \mathbf{W}_D^H \mathbf{D}_q^2 \mathbf{W}_D. \quad (16)$$

An alternate equivalent problem to (15) can be posed as

$$\begin{aligned} \mathbf{K} &= \alpha \mathbf{W}_D^H \mathbf{W}_A^H \mathbf{P} \Phi \mathbf{R} \mathbf{F}_A \mathbf{F}_D = \mathbf{I}_N, \\ \text{such that } \alpha^2 \sigma_n^2 \mathbf{W} \mathbf{W}^H + \mathbf{W}_D^H \mathbf{D}_q^2 \mathbf{W}_D &= \mathbf{0}. \end{aligned} \quad (17)$$

Both (15) and (17) are challenging to solve given the constraints on the analog precoder and combiner [32]. We take a multi-step approach to solve the problem by designing the hybrid precoder and combiner as a first step. In the next step, we derive the RIS phase setting, followed by fine-tuning the design of the digital precoder and combiner.

III. PRECODER AND COMBINER DESIGN

In order to design the precoders and combiners, we factor the digital precoder and combiner as

$$\mathbf{F}_D = \tilde{\mathbf{F}}_D \mathbf{F}_S, \quad \mathbf{W}_D^H = \mathbf{W}_S \tilde{\mathbf{W}}_D^H, \quad (18)$$

where $\tilde{\mathbf{F}}_D \in \mathbb{C}^{N \times M}$, $\mathbf{F}_S \in \mathbb{C}^{M \times N}$, $\tilde{\mathbf{W}}_D^H \in \mathbb{C}^{M \times N}$, and $\mathbf{W}_S \in \mathbb{C}^{N \times M}$. This is illustrated using Fig. 2. We first focus on designing the partial digital precoder $\tilde{\mathbf{F}}_D$ and partial digital combiner $\tilde{\mathbf{W}}_D^H$, and the analog precoder \mathbf{F}_A and analog combiner \mathbf{W}_A^H . We will later revisit the design of the other component of the digital precoder and combiner \mathbf{F}_S and \mathbf{W}_S in section IV-C.

The hybrid precoding and combining techniques for systems employing phase shifters in mmWave transceiver architectures impose constraints on them. The analog precoder \mathbf{F}_A and combiner \mathbf{W}_A^H entries need to satisfy unit norm entries in them [32]–[35]. We design the analog precoder \mathbf{F}_A and the partial digital precoder $\tilde{\mathbf{F}}_D$ such that

$$\mathbf{R} \mathbf{F}_A \tilde{\mathbf{F}}_D \approx \mathbf{I}_M. \quad (19)$$

The hybrid precoders are derived upon solving the optimization problem [33], [34] stated below.

$$(\mathbf{F}_A^{opt}, \tilde{\mathbf{F}}_D^{opt}) = \underset{\tilde{\mathbf{F}}_D, \mathbf{F}_A}{\operatorname{argmin}} \|\mathbf{R}^\dagger - \mathbf{F}_A \tilde{\mathbf{F}}_D\|_F, \quad (20)$$

$$\text{such that } \mathbf{F}_A \in \mathcal{F}_{RF}, \|\tilde{\mathbf{F}}_D \mathbf{F}_A\|_F^2 = N.$$

The set \mathcal{F}_{RF} is the set of all possible analog precoders that correspond to a hybrid precoder architecture based on phase shifters. This includes all possible $N_t \times N_{rt}$ matrices with constant magnitude entries. The term \mathbf{R}^\dagger denotes the right inverse of \mathbf{R} .

Similarly, the analog combiner \mathbf{W}_A^H and the partial digital combiner $\tilde{\mathbf{W}}_D^H$ are designed such that

$$\tilde{\mathbf{W}}_D^H \mathbf{W}_A^H \mathbf{P} \approx \mathbf{I}_M. \quad (21)$$

The hybrid combiners are derived using [34]

$$(\mathbf{W}_A^{Hopt}, \tilde{\mathbf{W}}_D^{Hopt}) = \underset{\tilde{\mathbf{W}}_D^H, \mathbf{W}_A^H}{\operatorname{argmin}} \|\mathbf{P}^\dagger - \tilde{\mathbf{W}}_D^H \mathbf{W}_A^H\|_F, \quad (22)$$

$$\text{such that } \mathbf{W}_A^H \in \mathcal{W}_{RF}, \|\tilde{\mathbf{W}}_D^H \mathbf{W}_A^H\|_F^2 = N.$$

Here again the set \mathcal{W}_{RF} is the set of all possible analog combiners that correspond to hybrid combiner architecture based on phase shifters. This includes all possible $N_{rs} \times N_r$ matrices with constant magnitude entries. The term \mathbf{P}^\dagger denotes the left inverse of \mathbf{P} .

IV. RIS PHASE SHIFT OPTIMIZATION

In this section, we derive the expression for the CRLB of the MSE of the received, quantized, and combined signal \mathbf{y} for a fixed \mathbf{W}_A^H , \mathbf{F}_A , $\tilde{\mathbf{W}}_D^H$, $\tilde{\mathbf{F}}_D$, and ADC bit resolution b on all the RF paths of the receiver, and show that the MSE achieves the CRLB. We later formulate an optimization problem to minimize the MSE (or CRLB) for RIS phase-shift setting. Finally, we describe a design to fine-tune the precoder \mathbf{F}_S and the combiner \mathbf{W}_S considering the optimal RIS phase-shift settings.

A. CRLB as function of RIS phase-shift settings

Given the analog combiner \mathbf{W}_A^H , analog precoder \mathbf{F}_A , the partial digital combiner $\tilde{\mathbf{W}}_D^H$, and the partial digital precoder $\tilde{\mathbf{F}}_D$ are derived using (20) and (22), we substitute them in (12) and rewrite the same as

$$\mathbf{y} = \mathbf{K} \mathbf{x} + \mathbf{n}_1, \quad (23)$$

where $\mathbf{K} = \alpha \mathbf{W}_S \Phi \mathbf{F}_S$, and $\mathbf{n}_1 = \alpha \mathbf{W}_S \tilde{\mathbf{W}}_D^H \mathbf{W}_A^H \mathbf{n} + \mathbf{W}_S \tilde{\mathbf{W}}_D^H \mathbf{n}_q$. We know that \mathbf{n} and \mathbf{n}_q are Gaussian random vectors such that $\mathbf{n} \sim \mathcal{N}(\mathbf{0}, \sigma_n^2 \mathbf{I}_{N_r})$ and $\mathbf{n}_q \sim \mathcal{N}(\mathbf{0}, \mathbf{D}_q^2)$ respectively. Hence we have

$$E[\mathbf{n}_1] = \alpha \mathbf{W}_S \tilde{\mathbf{W}}_D^H \mathbf{W}_A^H E[\mathbf{n}] + \mathbf{W}_S \tilde{\mathbf{W}}_D^H E[\mathbf{n}_q] = \mathbf{0}, \quad (24)$$

$$\sigma_{n_1}^2 = E[\mathbf{n}_1 \mathbf{n}_1^H] = \alpha^2 \sigma_n^2 \mathbf{W} \mathbf{W}^H + \mathbf{W}_S \tilde{\mathbf{W}}_D^H \mathbf{D}_q^2 \tilde{\mathbf{W}}_D \mathbf{W}_S^H. \quad (25)$$

Thus $\mathbf{n}_1 \sim \mathcal{N}(\mathbf{0}, (\alpha^2 \sigma_n^2 \mathbf{W} \mathbf{W}^H + \mathbf{W}_S \tilde{\mathbf{W}}_D^H \mathbf{D}_q^2 \tilde{\mathbf{W}}_D \mathbf{W}_S^H))$. It is noted that \mathbf{W} is an $N \times N_r$ matrix with $N_r \gg N$. It is safe to assume that \mathbf{W} has a full row rank and its pseudo-inverse exists. Equation (23) can be seen as a linear model, in which we intend to estimate \mathbf{x} , given the observation \mathbf{y} . We can express the conditional probability distribution of \mathbf{y} given \mathbf{x} as

$$p(\mathbf{y}|\mathbf{x}) \sim \frac{1}{(2\pi\sigma_{n_1}^2)^{\frac{N}{2}}} \exp\left\{-\frac{1}{2\sigma_{n_1}^2}(\mathbf{y} - \mathbf{K}\mathbf{x})^H(\mathbf{y} - \mathbf{K}\mathbf{x})\right\}. \quad (26)$$

From (23) and (26), it is straightforward to see that the ‘‘regularity conditions’’ are satisfied, and hence for such a linear estimator, we can write the expression for the CRLB as

$$\begin{aligned} \mathbf{I}^{-1}(\hat{\mathbf{x}}) &= (\mathbf{K}^H \mathbf{C}^{-1} \mathbf{K})^{-1} \\ &= \mathbf{F}_S^{-1} \left[\sigma_n^2 \Phi^{-1} \tilde{\mathbf{W}} \Phi + \frac{1}{\alpha^2} \Phi^{-1} \tilde{\mathbf{W}}_D^H \mathbf{D}_q^2 \tilde{\mathbf{W}}_D \Phi \right] (\mathbf{F}_S^H)^{-1}, \end{aligned} \quad (27)$$

where $\tilde{\mathbf{W}} = \tilde{\mathbf{W}}_D^H \mathbf{W}_A^H \mathbf{W}_A \tilde{\mathbf{W}}_D$, $\mathbf{D}_q^2 = \alpha(1 - \alpha) \text{diag} [(\tilde{\mathbf{W}}_D^H)^{-1} \Phi \mathbf{R} \mathbf{R}^H \Phi^{-1} \tilde{\mathbf{W}}_D^{-1} + \mathbf{I}_N]$, and \mathbf{C} the noise covariance matrix of \mathbf{n}_1 . The details of the proof are given in Appendix A.

It can also be seen that if the precoders, combiners, and the phase shift settings are designed such that $\mathbf{K} = \mathbf{I}_N$, the MSE in (16) achieves the CRLB. Formally,

$$\begin{aligned} \mathbf{I}^{-1}(\hat{\mathbf{x}}) &= \alpha^2 \sigma_n^2 \mathbf{W} \mathbf{W}^H + \mathbf{W}_S \tilde{\mathbf{W}}_D^H \mathbf{D}_q^2 \tilde{\mathbf{W}}_D \mathbf{W}_S^H, \\ &= \alpha^2 \sigma_n^2 \mathbf{W} \mathbf{W}^H + \mathbf{W}_D^H \mathbf{D}_q^2 \mathbf{W}_D, \\ &= \mathbf{M}(\mathbf{x}). \end{aligned} \quad (28)$$

B. Design of the RIS phase shift matrix

Minimizing the CRLB in (28) will ensure the minimum MSE (δ) performance for a given fixed \mathbf{W}_A^H , \mathbf{F}_A , $\tilde{\mathbf{W}}_D^H$, $\tilde{\mathbf{F}}_D$, and ADC bit resolution b . The CRLB (28) can be minimized when

$$\Phi^{-1} \tilde{\mathbf{W}}_D^H \left[\sigma_n^2 \mathbf{W}_A^H \mathbf{W}_A + \frac{1}{\alpha^2} \mathbf{D}_q^2 \right] \tilde{\mathbf{W}}_D \Phi = \mathbf{0}. \quad (29)$$

Thus the design of the RIS phase shift matrix can be posed as

$$\Phi^{opt} = \underset{\Phi}{\text{argmin}} \left\| \Phi^{-1} \tilde{\mathbf{W}}_D^H \left[\sigma_n^2 \mathbf{W}_A^H \mathbf{W}_A + \frac{1}{\alpha^2} \mathbf{D}_q^2 \right] \tilde{\mathbf{W}}_D \Phi \right\|_F^2. \quad (30)$$

It can also be shown further that minimizing (28) is equivalent to maximizing the throughput, and energy-efficiency of the wireless link. Please refer to Appendix B for the proofs.

C. Design of the partial digital precoder and combiner

Now we revisit the design of the other partial digital precoder \mathbf{F}_S and combiner \mathbf{W}_S . By substituting all the designed parameters into (17), we have

$$\mathbf{K} = \mathbf{W}_S \Phi^{opt} \mathbf{F}_S = \mathbf{I}_M. \quad (31)$$

By appropriately selecting a matrix \mathbf{F}_S^{opt} such that its right inverse $(\mathbf{F}_S^{opt})^\dagger$ exists we can rewrite (31) as

$$\mathbf{W}_S^{opt} = (\mathbf{F}_S^{opt})^\dagger (\Phi^{opt})^{-1}. \quad (32)$$

It is to be noted that $(\Phi^{opt})^H = (\Phi^{opt})^{-1}$ and the inverse $(\Phi^{opt})^{-1}$ always exists. In the next section we describe an algorithm to solve (30).

V. INFORMATION-DIRECTED BRANCH-AND-PRUNE ALGORITHM

In this section, we detail the proposed IDBP algorithm, which belongs to the family of tree-traversal search methods. The IDBP is very different compared from the existing tree-based algorithms. In it, we use an information-theoretic measure to decide on the branching and pruning rules during tree traversal to arrive at an optimal sequence or solution in probability. It is also vastly different compared to the well-known branch-and-bound algorithms [36], [37]. The difference between the two mainly is that in IDBP, the pruning decisions are not based on bounds of the reward or cost of the optimal solution, instead, they are based on an information-theoretic

measure. For the first time in the literature, we provide theoretical guarantees for near-optimality with the proposed IDBP algorithm using asymptotic equipartition theory.

A. The problem setup

We model the solution Φ as a sequence of random variables $\Phi = \{\Phi_1, \Phi_2, \dots, \Phi_M\}$, where we represent the discrete random variable Φ_i with probability mass function (PMF) $p(\Phi_i)$. The solution can be visualized as a finite horizon Markov decision process (MDP), which is defined using a tuple $(\Phi, \mathcal{A}, p, r, q)$, where Φ denotes the finite set of states, \mathcal{A} is the finite set of actions, $p : \Phi \times \mathcal{A} \times \Phi \rightarrow [0, 1]$ are the state transition probabilities $p_{\phi, a}(\phi')$ that a state ϕ' is attained when an action $a \in \mathcal{A}$ is taken in state ϕ where $\phi, \phi' \in \Phi$. A reward $r : \Phi \times \Phi \rightarrow \mathbb{R}$ is associated with an $a \in \mathcal{A}$ from a state $\phi \in \Phi$. The prior distribution q represents the statistic of the optimal solution. We consider the actions $a \in \mathcal{A}$ to be deterministic given p and q . We define a solution $\pi = \{\Phi_1 = \phi_1, \Phi_2 = \phi_2, \dots, \Phi_M = \phi_M\}$ as a sequence of states attained as a consequence of decisions $a \in \mathcal{A}$ taken to maximize the cumulative reward in the MDP. The details about the MDP assumption for the solution to (30) is detailed in Appendix C.

We design the IDBP algorithm with pruning rules so as to minimize the effective Kullback-Leibler (KL) divergence between the distribution of future looking sequence $\{\Phi_{m+1}, \dots, \Phi_M\}$ given Φ_m with respect to the known prior conditional distribution of the successive future states $q(\Phi_{m+1}, \Phi_{m+2}, \dots, \Phi_M | \Phi_m)$. We call this algorithm the IDBP. Effectively, we can write [38]

$$\pi^{opt} = \underset{\pi}{\text{argmin}} \{D_{KL}(p(\Phi_1, \dots, \Phi_M) || q(\Phi_1, \dots, \Phi_M))\}. \quad (33)$$

Using the Asymptotic Equipartition Property (AEP), it can be shown that the solution π^{opt} is optimal in probability. This is detailed in the next subsection. We say that the solution π^{opt} is close to π^* in probability when $Pr\{|f(\pi^{opt}) - f(\pi^*)| \leq \epsilon\} \geq 1 - \delta$, where ϵ, δ can be chosen arbitrarily close to zero. Here, π^* is the optimal solution to (30). That is $\Phi^{opt} = \text{diag}(\pi^*)$. Here $f(\cdot)$ is the objective function of (30), defined in (34).

B. Optimality Analysis

In this subsection, we provide the proofs of Theorems 1 - 3, and Lemma 1 that establishes theoretical guarantees of the optimal solution in probability using the proposed IDBP Algorithm. Before laying out the details of the optimality analysis, we first describe one of the methods that can be used to derive the statistics q .

1) *Determination of the priors of the optimal solution q* : Given that we model the solution as an MDP, we write the statistics of the optimal solution π^* as $\pi^* \sim q(\Phi_1, \Phi_2, \dots, \Phi_M)$, where $q(\Phi_1, \Phi_2, \dots, \Phi_M) = q(\Phi_1)q(\Phi_2|\Phi_1) \dots q(\Phi_M|\Phi_{M-1})$. Here $q(\Phi_1)$ is initial state distribution. We assume that the MDP is homogenous and hence it is sufficient to determine the transition probabilities

$q(\Phi_{t+1} = \phi_i | \Phi_t = \phi_j)$ between any two consecutive stages t and $t+1, \forall t \in [1, M]; \phi_i, \phi_j \in \Phi$. To do so, we identify m solutions $\{\pi^i\}_{i=1}^m$ from the exhaustive search space of problem (30) such that $f(\pi^1) \leq f(\pi^2) \leq \dots \leq f(\pi^m)$, where $f(\cdot)$ is the objective of the problem (30) written as $f(\pi) =$

$$\left\| \text{diag}(\pi)^{-1} \tilde{\mathbf{W}}_D^H \left[\sigma_n^2 \mathbf{W}_A^H \mathbf{W}_A + \frac{1}{\alpha^2} \mathbf{D}_q^2 \right] \tilde{\mathbf{W}}_D \text{diag}(\pi) \right\|_F^2. \quad (34)$$

Using these m subset of solutions we evaluate

$$q(\Phi_{t+1} = \phi_i | \Phi_t = \phi_j) = \frac{F(\{\Phi_{t+1} = \phi_i | \Phi_t = \phi_j\})}{mM} \quad (35)$$

$$\forall t \in [1, M]; \phi_i, \phi_j \in \Phi,$$

Here $F(\{\Phi_{t+1} = \phi_i | \Phi_t = \phi_j\})$ returns the number of times the event $\{\Phi_{t+1} = \phi_i | \Phi_t = \phi_j\}$ occur among the m solutions. It follows that if $\pi^* \in \{\pi^i\}_{i=1}^m$, and for a small m we have $q(\pi^*) \rightarrow 1$.

Alternatively, one can also use other fast non-parametric techniques or heuristic approaches to estimate the conditional priors q [39], [40].

We know that MDP $\Phi = \{\Phi_1, \Phi_2, \dots, \Phi_M\}$ can be visualized as homogenous Markov source, and exhibits asymptotic equipartition property. In addition, we also know the following [41], [42]

Definition 1. A sequence π_n (or a solution of length n) is strongly δ typical with respect to the distribution q if $\forall \phi \in \Phi : |q_{\pi_n}(\phi) - q(\phi)| \leq \delta q(\phi)$.

Here $q_{\pi_n}(\phi) = \frac{\ell(\phi)}{n}$ is the empirical distribution signifying the number of occurrences of ϕ denoted as $\ell(\phi)$ over n observations.

Definition 2. The strongly δ -typical set, $\mathcal{T}_\delta^n(\Phi)$ is a set of all strongly δ typical sequences. That is

$$\mathcal{T}_\delta^n(\Phi) = \left\{ \pi_n : \left| q_{\pi_n}(\phi) - q(\phi) \right| \leq \delta q(\phi) \right\}. \quad (36)$$

Definition 3. The weakly ϵ -typical set, $A_\epsilon^n(\Phi)$ is a set of all sequences such that

$$A_\epsilon^n(\Phi) = \left\{ \pi_n : \left| -\frac{1}{n} \log q(\pi_n) - H(\Phi) \right| \leq \epsilon \right\}, \quad (37)$$

where $H(\Phi)$ is the source entropy rate of the MDP under consideration. We now modify the Definition 1 to incorporate the conditional priors $q(\Phi_{t+1} = \phi_i | \Phi_t = \phi_j)$, and show that the solution π_n belongs to $A_\eta^n(\Phi)$, for some $\eta \rightarrow 0$, when the following condition $|q_{\pi_n}(\phi_i | \phi_j) - q(\phi_i | \phi_j)| \leq \delta q(\phi_i | \phi_j)$ is satisfied.

Theorem 1. A sequence π_n is η typical with respect to the conditional distribution q if $\forall \phi_i, \phi_j \in \Phi : |q_{\pi_n}(\phi_i | \phi_j) - q(\phi_i | \phi_j)| \leq \delta q(\phi_i | \phi_j)$, for some $\eta, \delta \rightarrow 0$.

Proof. We have $q_{\pi_n}(\phi_i | \phi_j)$ the empirical conditional distribu-

tion of the sequence π_n defined as

$$q_{\pi_n}(\Phi_{t+1} = \phi_i | \Phi_t = \phi_j) = q_{\pi_n}(\phi_i | \phi_j) = \frac{\ell(\{\phi_i | \phi_j\}; \pi_n)}{n},$$

$$\forall t \in [1, n); \phi_i, \phi_j \in \Phi, \quad (38)$$

where $\ell(\{\phi_i | \phi_j\}; \pi_n)$ denotes the number of occurrences of the transitions ϕ_i to ϕ_j in the sequence π_n . Let the sequence $\pi_n = \{\phi_{t(1)}, \phi_{t(2)}, \dots, \phi_{t(n)}\}$, where $\phi_{t(i)} \in \Phi, \forall i \in [1, n]$. Then we have

$$q(\pi_n) = q(\phi_{t(1)})^{\ell(\phi_{t(1)}; \pi_n)} \prod_{i=2}^{n-1} q(\phi_{t(i+1)} | \phi_{t(i)})^{\ell(\phi_{t(i+1)} | \phi_{t(i)}; \pi_n)}, \quad (39)$$

where $\ell(\phi_{t(1)}; \pi_n)$ is the number of occurrences of the state $\phi_{t(1)}$ in the sequence (solution) π_n . We write (39) as

$$\log(q(\pi_n)) = \ell(\phi_{t(1)}; \pi_n) \log q(\phi_{t(1)})$$

$$+ \sum_{i=2}^{n-1} \ell(\{\phi_{t(i+1)} | \phi_{t(i)}\}; \pi_n) \log q(\phi_{t(i+1)} | \phi_{t(i)}) \quad (40)$$

For simplicity of notation, we represent the conditionals $\{\phi_{t(i+1)} | \phi_{t(i)}\}$ as ψ_i , $\phi_{t(1)}$ as ψ_1 , and $\ell(\phi_{t(1)}; \pi_n)$ as $\ell(\psi_1)$. We simplify (40) further as

$$\log q(\pi_n) = \sum_{i=1}^{n-1} \ell(\psi_i) \log q(\psi_i),$$

$$= \sum_{i=1}^{n-1} \left\{ \ell(\psi_i) - nq(\psi_i) + nq(\psi_i) \right\} \log q(\psi_i),$$

$$= n \sum_{i=1}^{n-1} q(\psi_i) \log q(\psi_i)$$

$$+ n \sum_{i=1}^{n-1} \left(\frac{1}{n} \ell(\psi_i) - q(\psi_i) \right) \log q(\psi_i),$$

$$= -n \{ H(\Phi) + \eta \} \quad (41)$$

where $H(\Phi) = H(\Phi_1) + \sum_{i=2}^{N-1} H(\Phi_{i+1} | \Phi_i)$ for the MDP under consideration [41], and

$$\eta = \sum_{i=1}^{n-1} \left(\frac{1}{n} \ell(\psi_i) - q(\psi_i) \right) (-\log q(\psi_i)), \quad (42)$$

$$\leq \sum_{i=1}^{n-1} \frac{1}{n} \left| \ell(\psi_i) - nq(\psi_i) \right| (-\log q(\psi_i)).$$

We know that $\left| \frac{1}{n} \ell(\psi_i) - q(\psi_i) \right| = \left| q_{\pi_n}(\phi_i | \phi_j) - q(\phi_i | \phi_j) \right|$ for $i \in [1, n]$, and hence we have

$$\eta \leq \delta \sum_{i=1}^{n-1} q(\psi_i) (-\log q(\psi_i)) = \left| \delta H(\Phi) \right|, \text{ or} \quad (43)$$

$$\leq \hat{\eta}, \text{ where } \hat{\eta} = \left| \delta H(\Phi) \right|.$$

It is straightforward to see that for a finite $N, \hat{\eta} \rightarrow 0$ as $\delta \rightarrow 0$.

Hence we can write (42) as

$$\left(H(\Phi) - \hat{\eta}\right) \leq -\frac{1}{n} \log q(\pi_n) \leq \left(H(\Phi) + \hat{\eta}\right) \quad (44)$$

□

We now show that the optimal sequence $\pi^* \in A_\epsilon^M(\Phi)$.

Theorem 2. *Let q be the conditional priors derived using the m -best sequences $\{\pi^i\}_{i=1}^m$ as described in (35) that accurately represent the optimal solution π^* , then $\pi^* \in A_\epsilon^M(\Phi)$.*

Proof. Let the m -best sequences be denoted as

$$\pi^i = \{\phi_1^i, \phi_2^i, \dots, \phi_M^i\}, \text{ where } \phi_j^i \in \Phi, \forall j \in [1, M]. \quad (45)$$

we now have the empirical distribution of the sequences as

$$\begin{aligned} \hat{q}(\pi^i) &= \hat{q}_{\pi^i}(\phi_1^i) \prod_{j=2}^{M-1} \hat{q}_{\pi^i}(\phi_{j+1}^i | \phi_j^i), \\ \text{where } \hat{q}_{\pi^i}(\phi_1^i) &= \frac{\ell(\phi_1^i; \pi^i)}{M} = \frac{\ell(\{\phi_1^i | \phi_0\}; \pi^i)}{M}, \\ \hat{q}_{\pi^i}(\phi_{j+1}^i | \phi_j^i) &= \frac{\ell(\{\phi_{j+1}^i | \phi_j^i\}; \pi^i)}{M-1}. \end{aligned} \quad (46)$$

It is also worth noting that the starting transition ϕ_0 to ϕ_1^i occurs only once in the sequence. Hence in general we can write

$$\hat{q}_{\pi^i}(\phi_{j+1}^i | \phi_j^i) = \frac{\ell(\{\phi_{j+1}^i | \phi_j^i\}; \pi^i)}{M}. \quad (47)$$

However from (35) we have

$$q(\phi_{j+1} | \phi_j) = \frac{F(\phi_{j+1} | \phi_j)}{mM}. \quad (48)$$

Since $F(\phi_{j+1} | \phi_j)$ is the number of occurrences of the transitions ϕ_j to ϕ_{j+1} in all the m sequences, we can rewrite (47) as

$$\sum_{i=1}^m \hat{q}_{\pi^i}(\phi_{j+1}^i | \phi_j^i) = \frac{1}{M} \sum_{i=1}^m \ell(\phi_{j+1}^i | \phi_j^i; \pi^i) = \frac{1}{M} F(\phi_{j+1} | \phi_j). \quad (49)$$

We say that the empirical priors \hat{q} is an accurate representation of the optimal sequence π^* if

$$\begin{aligned} \hat{q}_{\pi^1}(\phi_{j+1} | \phi_j) &\approx \hat{q}_{\pi^2}(\phi_{j+1} | \phi_j) \approx \dots \approx \hat{q}_{\pi^m}(\phi_{j+1} | \phi_j) \\ &\approx \hat{q}_{\pi^*}(\phi_{j+1} | \phi_j) \forall j \in [1, M-1]. \end{aligned} \quad (50)$$

substituting (50) in (49) we have

$$\begin{aligned} m\hat{q}_{\pi^*}(\phi_{j+1} | \phi_j) &\approx \frac{1}{M} F(\phi_{j+1} | \phi_j), \\ \hat{q}_{\pi^*}(\phi_{j+1} | \phi_j) &\approx \frac{1}{mM} F(\phi_{j+1} | \phi_j), \\ \hat{q}_{\pi^*}(\phi_{j+1} | \phi_j) &\approx q(\phi_{j+1} | \phi_j), \forall j \in [1, M-1]. \end{aligned} \quad (51)$$

From (51) we can write

$$\begin{aligned} \left| \hat{q}_{\pi^*}(\phi_{j+1} | \phi_j) - q(\phi_{j+1} | \phi_j) \right| &\leq \delta q(\phi_{j+1} | \phi_j), \\ \forall j \in [1, M-1], \text{ and for some } \delta &\rightarrow 0. \end{aligned} \quad (52)$$

Now using Theorem 1 we can write $\pi^* \in A_\epsilon^M(\Phi)$ w.r.t conditional q ; if the statistic q is a close representation of

the optimal solution π^* . □

Using the proposed IDBP algorithm we find another sequence π^p as a solution, drawn from a conditional distribution $p(\phi_i | \phi_j), \forall i \in [1, M); \phi_i, \phi_j \in \Phi$ such that $p(\pi^p) \approx q(\pi^*)$, and $D_{KL}(p||q) \rightarrow 0$. We now show that the sequences $\pi^p, \pi^* \in A_\eta^M(\Phi)$ w.r.t the conditional q for some $\eta \rightarrow 0$.

Theorem 3. *Let π^p be a sequence obtained using the conditional distribution $p(\phi_i | \phi_j)$ such that $p_{\pi^p}(\phi_i | \phi_j) \approx q_{\pi^*}(\phi_i | \phi_j), \phi_i, \phi_j \in \Phi$, and $D_{KL}(p||q) \rightarrow 0$; then it can be shown that the sequence π^p and π^* belong to the typical set w.r.t the conditional q . That is $\pi^p, \pi^* \in A_\eta^M(\Phi)$ for some $\eta \rightarrow 0$.*

Proof. We have

$$p_{\pi^p}(\phi_i | \phi_j) \approx q_{\pi^*}(\phi_i | \phi_j), \forall \phi_i, \phi_j \in \Phi, D_{KL}(p||q) \rightarrow 0. \quad (53)$$

From Theorem 2, we have $\pi^* \in A_\epsilon^M(\Phi)$, and using Theorem 1 we can write

$$\begin{aligned} \left| q_{\pi^*}(\phi_i | \phi_j) - q(\phi_i | \phi_j) \right| &\leq \delta q(\phi_i | \phi_j), \text{ or} \\ \left| p_{\pi^p}(\phi_i | \phi_j) - q(\phi_i | \phi_j) \right| &\leq \delta' q(\phi_i | \phi_j). \text{ (using (53))} \end{aligned} \quad (54)$$

where $\delta' \rightarrow 0$. For some $\eta = \max(\delta, \delta')$, we can write the following

$$\begin{aligned} \left| p_{\pi^p}(\phi_i | \phi_j) - q(\phi_i | \phi_j) \right| &\leq \eta q(\phi_i | \phi_j), \\ \left| q_{\pi^*}(\phi_i | \phi_j) - q(\phi_i | \phi_j) \right| &\leq \eta q(\phi_i | \phi_j), \end{aligned} \quad (55)$$

where $\eta \rightarrow 0$, and $\forall \phi_i, \phi_j \in \Phi$. Hence we have $\pi^p, \pi^* \in A_\eta^M(\Phi)$. □

Finally, it follows that if $\pi^p \in A_\eta^M(\Phi)$ w.r.t the conditional q , which is a close representation of π^* , then π^p is optimal solution in probability.

Lemma 1. *If $\pi^p, \pi^* \in A_\eta^M(\Phi)$ w.r.t the conditionals q , and if q is a close representation of the optimal solution π^* we have $\Pr\left\{ |f(\pi^{opt}) - f(\pi^*)| \leq \epsilon \right\} \geq 1 - \delta$, where ϵ, δ are very small numbers not related to η .*

Proof. Since we have $\pi^p, \pi^* \in A_\eta^M(\Phi)$, we have

$$\begin{aligned} p(\pi^p) &= p(\pi^*) \approx 1, \text{ or } \pi^p \rightarrow \pi^*; \text{ Hence we can safely write} \\ \Pr\left\{ |f(\pi^{opt}) - f(\pi^*)| \leq \epsilon \right\} &\geq 1 - \delta. \end{aligned} \quad (56)$$

□

VI. ALGORITHM DESCRIPTION

Inspired by the well-known Chow-Liu Algorithm (CLA), we develop the proposed IDBP algorithm to arrive at the solution π^{opt} [43]. The CLA minimizes the KL divergence between the actual distribution represented using the conditional priors q and the distribution of π^{opt} . It finds the best second-order product approximation of the multi-dimensional discrete probability distribution from a finite set of observed data. The CLA finds the optimal tree-structured network $T(X_1, X_2, \dots, X_k)$

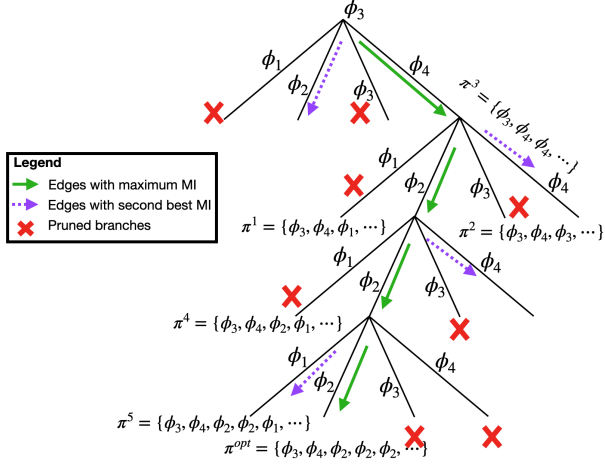


Fig. 3: An illustration of the tree traversal using the proposed IDBP Algorithm.

of depth k by minimizing the KL divergence between the observed (actual) distribution $p_t(X_1, X_2, \dots, X_k)$ and the tree-structured distribution $T(X_1, X_2, \dots, X_k)$. That is

$$\min_T \{D_{KL}(p_t(X_1, \dots, X_k) || T(X_1, \dots, X_k))\}, \quad (57)$$

where $\{X_1, X_2, \dots, X_k\}$ is a sequence of random variables. One of the key results from [43] is that, for minimizing the KL divergence in (57), it is sufficient to find a tree network T such that we maximize the mutual information (MI) $I(X_i, X_{\gamma(i)})$ between the tree edges in T . Here $X_{\gamma(i)}$ denotes the parent of X_i in the tree under consideration.

The proposed IDBP algorithm maximizes the MI between the tree edges (branches) to select the optimal-path edges and prune others. This ensures optimal solution in probability to (30). It is also worth noting that since we have an MDP model for our solution, it suffices to consider a second-order approximation for the joint probability distribution. Given the prior statistics q of the optimal solution, and the transition probabilities p between the phase settings, we traverse the tree by maintaining the edges that maximize the MI $I(X_i, X_{\gamma(i)})$. The proposed IDBP algorithm is described using Algorithm 2. The algorithm yields an optimal solution in probability π^{opt} if the priors q selected is a close representation of the optimal solution π^* . In such a situation, the proposed IDBP algorithm requires a single pass tree traversal to get to the solution π^{opt} . This is the best case. However, in situations when q is not an accurate representation of π^* , we propose to use a second pass from every node visited to traverse the tree along with the second-best child. This is described in Algorithm 2. One can choose to extend the algorithm to explore k -best children. An illustration of the proposed IDBP tree search is shown in Fig. 3. However, when extended to all the children, the algorithm becomes an exhaustive search. The process of designing the hybrid precoder, hybrid combiner, and the RIS phase configuration is outlined as design flow in Algorithm 1.

Algorithm 1 Design flow

```

1: procedure DESIGN FLOW
2:    $\{\mathbf{F}_A^{opt}, \tilde{\mathbf{F}}_D^{opt}\} \leftarrow$  using (20)
3:    $\{\mathbf{W}_A^{Hopt}, \tilde{\mathbf{W}}_D^{Hopt}\} \leftarrow$  using (22)
4:    $\Phi^{opt} \leftarrow$  by solving (30) using IDBP
5:    $\{(\mathbf{F}_S^{opt}), (\mathbf{W}_S^{opt})\} \leftarrow$  using (31) and (32)
6:   return  $\{\mathbf{F}_A^{opt}, \mathbf{W}_D^{opt}, \Phi^{opt}, \Phi^{opt}, \mathbf{F}_S^{opt}, \mathbf{W}_S^{opt}\}$ 
7: end procedure

```

Algorithm 2 Proposed IDBP

```

1: function IDBP( $\Phi, M, m$ )
2:    $\Phi \leftarrow$  Finite set of phase angles with cardinality  $K$ 
3:    $M \leftarrow$  Number of RIS elements
4:    $m \leftarrow$  Number of sequences used to derive the priors  $q$ 
5:   InitializeStack()
6:    $\pi^{opt} \leftarrow \emptyset; C_{opt} \leftarrow \infty$ 
7:    $q \leftarrow$  Compute the priors as described in Section V-B1
8:    $p \leftarrow$  Compute the initial state probabilities
9:    $X_0 \leftarrow$  Compute using  $p$  and  $q$ 
10:   $c \leftarrow$  Compute initial cost using  $p$  and  $q$ 
11:   $\pi^{opt} \leftarrow$  TraverseTree( $X_0, c, p, q, M, 2, 1$ )
12:  return  $\{\pi^{opt}\}$  ▷ Solution
13: end function
14: function TRAVERSE TREE( $X_{curr}, c, p, q, M, stage, rec$ )
15:   $X_{curr} \leftarrow$  Current node in the tree
16:   $r \leftarrow$  Accumulated cost up till the node  $X_{curr}$ 
17:   $q \leftarrow$  The conditional priors
18:   $p \leftarrow$  The transition probabilities
19:   $M \leftarrow$  Number of RIS elements
20:   $stage \leftarrow$  The current stage(level) in the tree traversal
21:   $rec \leftarrow$  Indicator to control recursion
22:  if  $stage > M$  then
23:    Get the traversed sequence and its
24:    accumulated cost
25:     $\{\pi^p, f(\pi^p)\} \leftarrow$  ReadStack() ▷ refer (34).
26:    if  $f(\pi^p) \leq C_{opt}$  then
27:       $\pi^{opt} \leftarrow \pi^p$ 
28:       $C_{opt} \leftarrow f(\pi^p)$ 
29:    end if
30:    pop() and return
31:  end if
32:   $\{X_{c1}, X_{c2}, C_{c1}, C_{c2}\} \leftarrow$  findBestChildren( $X_{curr}, c, p$ )
33:  Push( $X_{c1}, C_{c1}, stage$ )
34:  TraverseTree( $X_{c1}, C_{c1}, p, q, M, stage+1, rec$ )
35:  if  $rec = 1$  then
36:    Push( $X_{c2}, C_{c2}, stage$ )
37:    TraverseTree( $X_{c2}, C_{c2}, p, q, M, stage+1, 0$ )
38:  end if
39:  pop() and return
40: end function
41: function FINDBESTCHILDREN( $X_{curr}, c, p$ )
42:   $X_{curr} \leftarrow$  The current node in the tree being processed
43:   $c \leftarrow$  Running cost of the sequence
44:   $p \leftarrow$  The transition statistics
45:  for each child  $X_i$  of the current node  $X_{curr}$  do
46:     $c(i) \leftarrow c(i) + p(X_i, X_{curr}) \log_2 \frac{p(X_i, X_{curr})}{p(X_i)p(X_{curr})}$ 
47:  end for
48:   $\{I_1, I_2\} \leftarrow argmax(c)$ 
49:  Return two best children and their running cost.
50:  return  $\{X_{I_1}, X_{I_2}, c(I_1), c(I_2)\}$ 
51: end function

```

VII. COMPUTATIONAL COMPLEXITY ANALYSIS

The algorithm yields an optimal solution in probability π^{opt} if the priors q selected is a close representation of the optimal solution π^* . In such a situation, the proposed IDBP algorithm requires a single-pass tree traversal to get to the solution π^{opt} . This is the best case. However, when q is not an accurate representation of π^* , additional solutions can be explored using a second pass from every node visited by traversing the tree along the second-best child. Although following the path along second-best child recursively explores more solutions, it is easy to see that this increases the complexity exponentially in M , having a time complexity of $\approx O(2^M)$. The algorithm will turn out to be an ES if one has to follow K -best paths recursively having a complexity of $O(K^M)$. Alternatively, we propose to follow k -best children, but not recursively. A 2-best children solution exploration in a non-recursive fashion is described in Algorithm 2. One can choose to extend this algorithm to explore k -best children. This is illustrated using Fig.4.

A single-pass tree traversal to get to the solution π^{opt} has a complexity of $O(\mu KM)$, where M is the number of RIS elements (also the depth of the tree under consideration). The term μ is the number of arithmetic operations required to compute the MI between the current node and one of its children. Hence to compute the MI between a given node and all its children, the number of arithmetic operations required is μK , where K is the cardinality of Φ . When exploring additional solutions using a second pass from every node visited (in a non-recursive fashion) to traverse the tree along the second-best child, the number of nodes to be processed is $M + 1 + 2 + \dots + M - 1 = \frac{M(M+1)}{2}$, and hence has a complexity of $O(\mu KM^2)$. This is illustrated in Fig.4. Similarly, when we consider solutions from the 3-best children along the best-child path, the number of nodes to be processed is $M + 2 + 4 + \dots + 2(M - 1) = M + 2 \frac{M(M-1)}{2}$, which again has $O(\mu KkM^2)$ complexity. In general, solutions considering k -best children along the best-child path have a complexity of $O(\mu KkM^2)$. Extending the result to explore

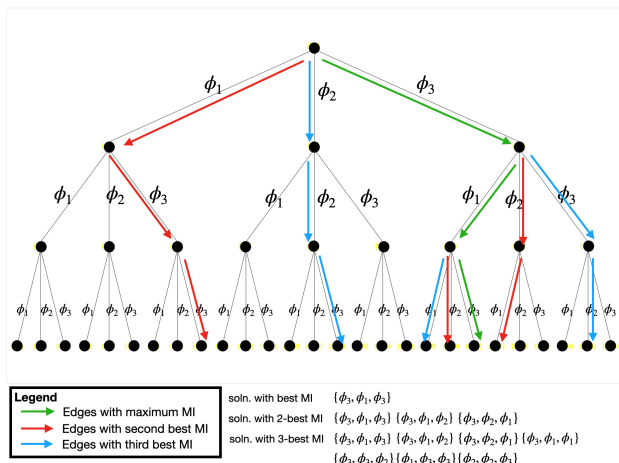


Fig. 4: An illustration of the path (solutions) explored when using a single-pass, 2–best, and 3–best children traversal.

K -best solutions from the best path still has a polynomial-time computational complexity of $O(\mu K^2 M^2)$. On average, with a prior q selected to have a close statistics of the optimal solution π^* , the proposed IDBP algorithm yields an optimal solution in probability π^{opt} with a complexity of $O(\mu K^2 M^2)$. One of the many ways to identify the priors q to have a good representation of π^* is to use a fast heuristic algorithm to identify $\{\pi^i\}_{i=1}^m$ discussed in subsection V-B1 [44]. It is to be noted that this computational complexity does not include the evaluation of the conditional priors q described in V-B1. The priors q can be evaluated with significantly reduced computation using random sampling (with $m \ll M$) or heuristics methods [39], [40].

The TMH algorithm proposed in [19] requires the computation of the matrix \mathbf{K} , and finding its eigenvector that corresponds to its maximum eigenvalue as described using (11) and (12) in Section III-A of [19]. The resultant eigenvector quantized to the nearest possible discrete angles yields the solution. To compute the matrix \mathbf{K} the effective number of multiplications are $N_t N_r M^2$. Finding the required eigenvector has a complexity of $O(M^3)$, assuming no structure about the matrix \mathbf{K} , which is a reasonable assumption. This results in the computational complexity of TMH to be $O(M^3)$.

The complexity of the reflecting schemes $eMSE$ R and $vMSE$ R proposed in [24] is shown to be $\approx O(L^{2N} K^2)$. Here L corresponds to the L -ary QAM symbols used. The discussion is summarized in the Table I.

Algorithm	Computational complexity	Matlab runtime* for $M = 12$
ES	$O(K^M)$	415.5
Proposed IDBP	$\approx O(KM)$ §	18.3
Proposed IDBP	$\approx O(K^2 M^2)$ †	18.8
TMH [◇]	$\approx O(M^3)$	56
AO1 [◇] ($eMSE$ R-Reflecting)	$\approx O(L^{2N} K^2) / O(L^{2N} K^3)$	228
AO2 [◇] ($vMSE$ R-Reflecting)	$\approx O(L^{2N} K^2) / O(L^{2N} K^3)$	345

§ conditional priors q is a close representation of the solution π^* ,

† conditional priors q not a close representation of the solution π^* .

◇ refer to Section VIII (Simulations).

*The matlab runtime (in secs.) includes precoder, combiner, RIS evaluations, and prior evaluation at a given SNR.

TABLE I: Computational complexity comparison.

VIII. SIMULATIONS

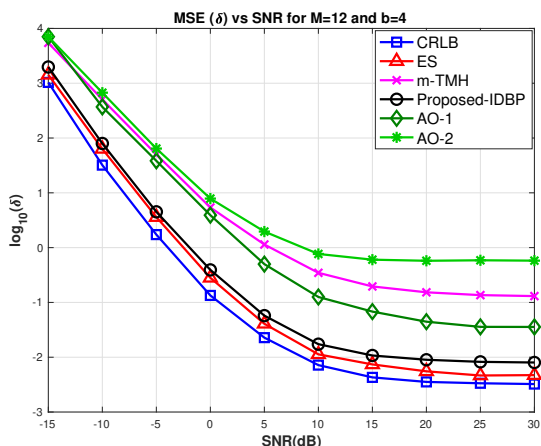
In this section, we first compare the following algorithms- (i) the exhaustive search (ES) method to solve the (30), (ii) the proposed IDBP algorithm to solve (30) (IDBP), (iii) the exhaustive search to solve the trace maximization (TM) framework considering the diagonal RIS architecture proposed in [19] (m-TMH), and the AO algorithm proposed in [24]. The evaluation of the ES for RIS elements when $M > 12$, and with the phase-shift settings $K \geq 3$ becomes impractical. Hence, for this evaluation, we only consider the case where $M = 12$ with the ADC bit resolution set to $b = 4$ on all the RF paths of the receiver. The other configurations parameters used for this evaluation are presented in Table II. The channel model for \mathbf{P} and \mathbf{R} are derived using the multi-user interference model discussed in Section II considering eight ($\beta = 8$) strong RIS reflected interference and one non-RIS reflected interferer. The detailed analysis of such a

multi path propagation environment is described in Section II-B of [19]. The AO algorithm encompasses the combiner in addition to precoder and RIS that is discussed in [24]. The algorithm is described in Appendix D. The convergence of the AO algorithm is strongly dependent on the selection of the initial solutions and hence we consider two scenarios of AO with different initial solutions (AO1 and AO2). The initial solutions for AO1 and AO2 are chosen empirically. We run the simulations considering the above parameters to evaluate the MSE, using which we compute the information rate of the link as

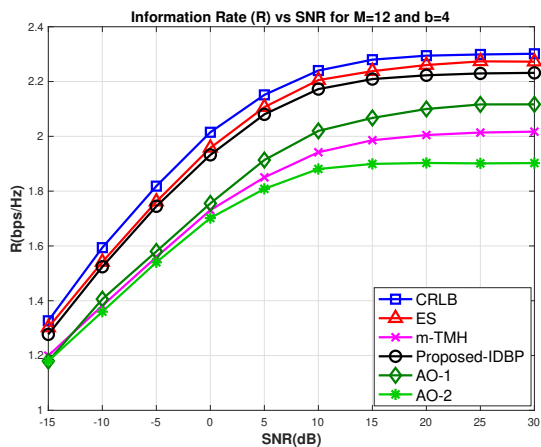
$$R(\Phi) = N \log_2 p + \log_2 \det \left((\mathbf{M}(\mathbf{x}))^{-1} + \frac{1}{p} \mathbf{I}_N \right). \quad (58)$$

The proof of (58) is detailed in Appendix B. The simulation results obtained are shown in Fig. 5. From Fig. 5, it can be observed that the ES achieves the CRLB for the given (designed) hybrid precoders and combiners. The proposed IDBP algorithm, which is a computationally efficient method to solve (30), extracts a near-optimal solution that is close to ES and has a superior performance compared to both the

trace-maximization algorithm (m-TMH) proposed in [19], and AO1 and AO2 based on [24]. Subsequently, we run simulations with $M = 64, 128$, and 256 to compare the following algorithms- (i) the proposed IDBP algorithm to solve (30) (IDBP), (ii) optimal trace maximization (TMH) method called the diagonal Φ (OPT-DIAG) [19], and (iii) alternating optimization (AO1) based on the work in [24]. The TMH is a computationally efficient algorithm to solve the trace maximization proposed in [19]. The details of this algorithm are presented in the Section III-A of [19]. We evaluate the MSE and the information rate R for SNRs in the range $[-30, 30]$ dB in steps of 5dB and for ADC bits $b = 2, 3$, and 4 on all the RF paths. The results obtained are shown using the Fig.6, Fig.7, and Fig.8 for $M = 64, 128$, and 256 , respectively. From the results, it can be observed that the proposed IDBP algorithm outperforms both the TMH and the AO methods.



(a) MSE performance.



(b) Information rate performance.

Fig. 5: MSE and information rate at various SNRs with proposed IDBP, TMH, AO, and the ES method with the number of RIS elements $M = 12$ for ADC bits $b = 4$ on all RF paths.

Parameters	Value/Type
Frequency	28Ghz
Environment	Non Line of sight (NLOS)
Tx-Rx seperation	100m
Tx-RIS seperation	70m
RIS-Rx seperation	70m
TX/RX array type	ULA
Num of TX/RX elements N_t/N_r	48/48
TX/RX antenna spacing	$\lambda/2$
Number of Passive RIS elements (M)	12,64,128,256
Number of discrete phase settings (K)	$\{\frac{25\pi}{36}, \frac{73\pi}{36}, \frac{49\pi}{36}\}$
ADC bit resolution on all RF paths (b)	2,3,4
Number of RF paths at TX and RX (N)	8
Signal bandwidth	100Mhz
Sampling Frequency	400Mhz
Modulation Type	64 QAM
Number of symbols	200
Number of interferer paths (β)	8

TABLE II: The configuration parameters used for our simulations.

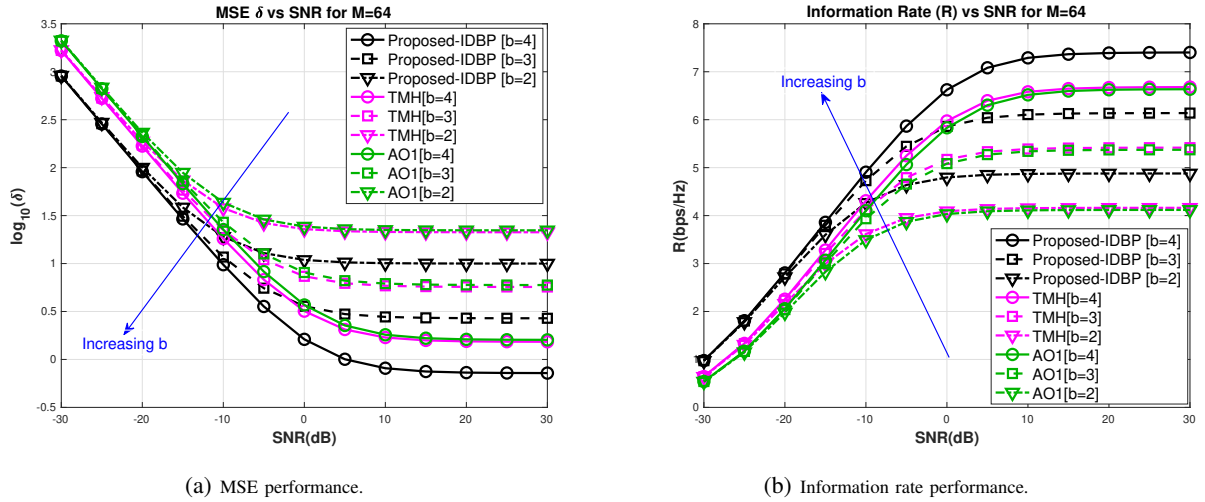


Fig. 6: MSE and information rate at various SNRs with proposed IDBP, TMH, and AO algorithms with the number of RIS elements $M = 64$, and for b -bit ADC in all of the receiver paths.

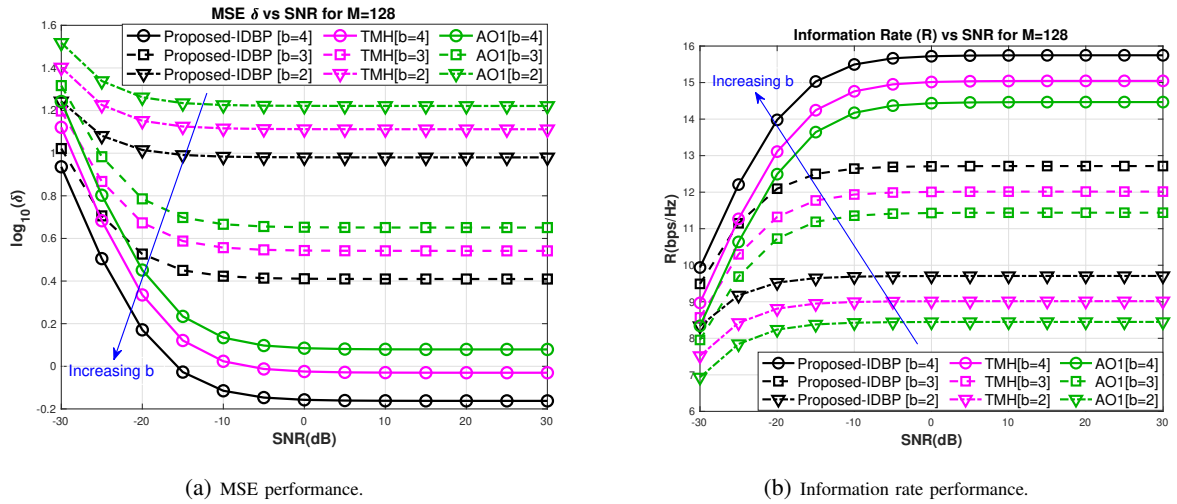


Fig. 7: MSE and information rate at various SNRs with proposed IDBP, TMH, and the AO algorithms with the number of RIS elements $M = 128$, and for b -bit ADC in all of the receiver paths.

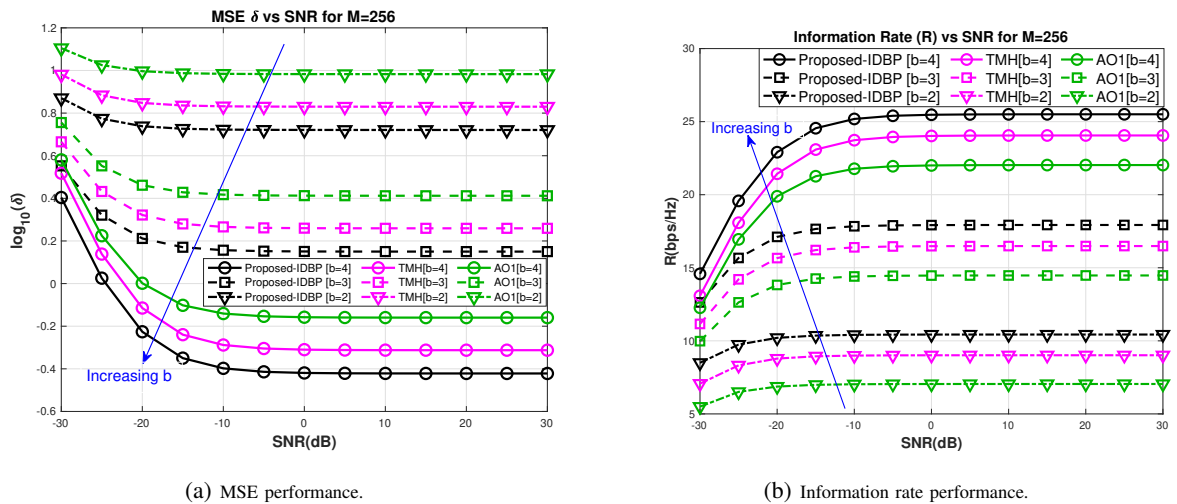


Fig. 8: MSE and information rate at various SNRs with proposed IDBP, TMH, and the AO algorithms with the number of RIS elements $M = 256$, and for b -bit ADC in all of the receiver paths.

IX. CONCLUSION

The discrete phase optimization algorithm for a passive-RIS that assists a multi-user MaMIMO communication system under interference is studied in this paper. A novel algorithm based on an information-theoretic tree search called IDBP is proposed in this work. We developed the theoretical framework for this proposed algorithm using the Asymptotic Equipartition Property, and establish near-optimality guarantees. We discuss a method to design hybrid precoders and combiners along with RIS phase configuration to minimize the MSE of a blocked LOS link assisted by a RIS and show that it achieves the Cramer-Rao Lower-Bound. We consider the MaMIMO receivers to be equipped with low-resolution ADCs. We also show minimizing the MSE and maximizing the throughput of a blocked LOS link under interference are equivalent. Using simulation, we compare the proposed algorithm with the exhaustive search and two other state-of-the-art algorithms and demonstrate that the proposed method outperforms the state-of-the-art with significant computational savings with an appropriate selection of the prior distribution. This makes it more suitable for the proposed algorithm to be used with RIS having a large number of elements M and a large number of configurable discrete phase settings K . The typical use cases of such scenarios are in vehicular and cellular backhaul wireless communication links.

REFERENCES

- [1] Q. Wu, S. Zhang, B. Zheng, C. You, and R. Zhang, "Intelligent reflecting surface-aided wireless communications: A tutorial," *IEEE Transactions on Communications*, vol. 69, no. 5, pp. 3313–3351, 2021.
- [2] d. Jiang and L. Delgrossi, "Ieee 802.11p: Towards an international standard for wireless access in vehicular environments," *2008 IEEE Vehicular Technology Conference*, pp. 2036–2040, 2008.
- [3] Z. Ali, S. Lagn, L. Giupponi, and R. Rouil, "3gpp nr v2x mode 2: Overview, models and system-level evaluation," *IEEE Access*, vol. 9, pp. 89 554–89 579, 2021.
- [4] S. Busari, M. Khan, K. Saidul Huq, S. Mumtaz, and J. Rodriguez, "Millimetre wave massive mimo for cellular vehicle-to-infrastructure communication," *IET Intelligent Transport Systems*, vol. 13, no. 6, pp. 983–990, 2019.
- [5] Y. Chen, Y. Wang, J. Zhang, and Z. Li, "Resource allocation for intelligent reflecting surface aided vehicular communications," *IEEE Transactions on Vehicular Technology*, vol. 69, no. 10, pp. 12 321–12 326, 2020.
- [6] D. Dampahalage, K. B. Shashika Manosha, N. Rajatheva, and M. Latva-aho, "Intelligent reflecting surface aided vehicular communications," pp. 1–6, 2020.
- [7] A. Al-Hilo, M. Samir, M. Elhattab, C. Assi, and S. Sharafeddine, "Reconfigurable intelligent surface enabled vehicular communication: Joint user scheduling and passive beamforming," *IEEE Transactions on Vehicular Technology*, vol. 71, no. 3, pp. 2333–2345, 2022.
- [8] D. Prez-Adn, . Fresnedo, J. P. Gonzalez-Coma, and L. Castedo, "Intelligent reflective surfaces for wireless networks: An overview of applications, approached issues, and open problems," *Electronics*, vol. 10, no. 19, 2021.
- [9] Y. Liang, J. Chen, R. Long, Z. He, X. Lin, X. Lin, C. Huang, S. Liu, X. S. Shen, and M. D. Renzo, "Reconfigurable intelligent surfaces for smart wireless environments: channel estimation, system design and applications in 6g networks," *Science China Information Sciences*, vol. 64, 2021.
- [10] S. Yan, X. Zhao, D. W. K. Ng, J. Yuan, and N. Al-Dhahir, "Intelligent reflecting surface for wireless communication security and privacy," *CoRR*, vol. abs/2103.16696, 2021. [Online]. Available: <https://arxiv.org/abs/2103.16696>
- [11] Y. Yang, B. Zheng, S. Zhang, and R. Zhang, "Intelligent reflecting surface meets ofdm: Protocol design and rate maximization," *IEEE Transactions on Communications*, vol. 68, no. 7, pp. 4522–4535, 2020.
- [12] Z. Ding and H. Vincent Poor, "A simple design of irts-noma transmission," *IEEE Communications Letters*, vol. 24, no. 5, pp. 1119–1123, 2020.
- [13] H. A. U. Mustafa, M. A. Imran, M. Z. Shakir, A. Imran, and R. Tafazolli, "Separation framework: An enabler for cooperative and d2d communication for future 5g networks," *IEEE Communications Surveys Tutorials*, vol. 18, no. 1, pp. 419–445, 2016.
- [14] B. Tahir, S. Schwarz, and M. Rupp, "Ris-assisted code-domain mimo-noma," *2021 29th European Signal Processing Conference (EUSIPCO)*.
- [15] Y. Liu, X. Mu, R. Schober, and H. V. Poor, "Simultaneously transmitting and reflecting (star)-riss: a coupled phase-shift model," *ICC 2022 - IEEE International Conference on Communications*, pp. 2840–2845, 2022.
- [16] X. Guo, Y. Chen, and Y. Wang, "Learning-based robust and secure transmission for reconfigurable intelligent surface aided millimeter wave uav communications," *IEEE Wireless Communications Letters*, vol. 10, no. 8, pp. 1795–1799, 2021.
- [17] S. Zhang, H. Zhang, B. Di, Y. Tan, Z. Han, and L. Song, "Beyond intelligent reflecting surfaces: Reflective-transmissive metasurface aided communications for full-dimensional coverage extension," *IEEE Transactions on Vehicular Technology*, vol. 69, no. 11, pp. 13 905–13 909, 2020.
- [18] Y. Xiu, J. Zhao, E. Basar, M. D. Renzo, W. Sun, G. Gui, and N. Wei, "Uplink achievable rate maximization for reconfigurable intelligent surface aided millimeter wave systems with resolution-adaptive adcs," *IEEE Wireless Communications Letters*, vol. 10, no. 8, pp. 1608–1612, 2021.
- [19] A. M. Sayeed, "Optimization of reconfigurable intelligent surfaces through trace maximization," *2021 IEEE International Conference on Communications Workshops (ICC Workshops)*, pp. 1–6, 2021.
- [20] Y. Omid, S. M. Mahdi Shahabi, C. Pan, Y. Deng, and A. Nallanathan, "A trellis-based passive beamforming design for an intelligent reflecting surface-aided miso system," *IEEE Communications Letters*, pp. 1–1, 2022.
- [21] B. Zheng, Q. Wu, and R. Zhang, "Intelligent reflecting surface-assisted multiple access with user pairing: Noma or oma?" *IEEE Communications Letters*, vol. 24, no. 4, pp. 753–757, 2020.
- [22] X. Yu, D. Xu, and R. Schober, "Optimal beamforming for miso communications via intelligent reflecting surfaces," *2020 IEEE 21st International Workshop on Signal Processing Advances in Wireless Communications (SPAWC)*, pp. 1–5, 2020.
- [23] Q. Wu and R. Zhang, "Beamforming optimization for wireless network aided by intelligent reflecting surface with discrete phase shifts," *IEEE Transactions on Communications*, vol. 68, no. 3, pp. 1838–1851, 2020.
- [24] J. Y and M. S. Alouini, "Joint reflecting and precoding designs for ser minimization in reconfigurable intelligent surfaces assisted mimo systems," *IEEE Transactions on Wireless Communications*, vol. 19, no. 8, pp. 5561–5574, 2020.
- [25] S. Gong, Z. Yang, C. Xing, J. An, and L. Hanzo, "Beamforming optimization for intelligent reflecting surface-aided swipt iot networks relying on discrete phase shifts," *IEEE Internet of Things Journal*, vol. 8, no. 10, pp. 8585–8602, 2021.
- [26] A. V. Savkin, C. Huang, and W. Ni, "Joint multi-uav path planning and los communication for mobile edge computing in iot networks with riss," *IEEE Internet of Things Journal*, pp. 1–1, 2022.
- [27] D. W. Yue, H. H. Nguyen, and Y. Sun, "mmwave doubly-massive-mimo communications enhanced with an intelligent reflecting surface: asymptotic analysis," *IEEE Access*, vol. 8, pp. 183 774–183 786, 2020.
- [28] D. W. Yue and H. H. Nguyen, "Multiplexing gain analysis of mmwave massive mimo systems with distributed antenna subarrays," *IEEE Transactions on Vehicular Technology*, vol. 68, no. 11, pp. 11 368–11 373, 2019.
- [29] O. E. Ayach, R. W. Heath, S. Abu-Surra, S. Rajagopal, and Z. Pi, "The capacity optimality of beam steering in large millimeter wave mimo systems," *IEEE 13th International Workshop on Signal Processing Advances in Wireless Communications (SPAWC)*, pp. 100–104, 2012.
- [30] O. Orhan, E. Erkip, and S. Rangan, "Low power analog-to-digital conversion in millimeter wave systems: Impact of resolution and bandwidth on performance," *2015 Information Theory and Applications Workshop (ITA)*, pp. 191–198, Feb 2015.
- [31] Li Fan, Shi Jin, Chao-Kai Wen, and Haixia Zhang, "Uplink achievable rate for massive MIMO systems with low resolution ADC," *IEEE Commun. Letters*, vol. 19, no. 12, pp. 2186–2189, Oct. 2015.
- [32] I. Z. Ahmed, H. R. Sadjadpour, and S. Yousefi, "An optimal low-complexity energy-efficient adc bit allocation for massive mimo," *IEEE Transactions on Green Communications and Networking*, vol. 5, no. 1, pp. 61–71, 2021.

- [33] R. W. Heath, N. Gonzalez-Prelcic, S. Rangan, W. Roh, and A. M. Sayeed, "An overview of signal processing techniques for millimeter wave mimo systems," *IEEE Journal of Selected Topics in Signal Processing*, vol. 10, no. 3, pp. 436–453, April 2016.
- [34] Omar El Ayach, Sridhar Rajagopal, Shadi Abu-Surra, Zhouyue Pi, Robert W. Heath Jr., "Spatially sparse precoding in millimeter wave MIMO systems," *IEEE Journ. in Selected Areas of Comm.*, vol. 8, no. 3, 2017.
- [35] I. Z. Ahmed, H. Sadjadpour, and S. Yousefi, "Single-user mmwave massive MIMO: Svd-based adc bit allocation and combiner design," *SPCOM-2018*, pp. 357–361, July 2018.
- [36] D. R. Morrison, S. H. Jacobson, J. J. Sauppe, and E. C. Sewell, "Branch-and-bound algorithms," *Discret. Optim.*, vol. 19, pp. 79–102, Feb. 2016.
- [37] S. Z. Boyd and J. Mattingley, "Branch and bound methods," 2003.
- [38] N. Tishby and D. Polani, "Information theory of decisions and actions," *Perception-Action Cycle. Springer Series in Cognitive and Neural Systems*. Springer, New York, NY, 2011.
- [39] M. P. Holmes, A. G. Gray, and C. L. Isbell, "Fast nonparametric conditional density estimation," *Proceedings of the Twenty-Third Conference on Uncertainty in Artificial Intelligence*, p. 175182, 2007.
- [40] D. B. Huberman, B. J. Reich, and H. D. Bondell, "Nonparametric conditional density estimation in a deep learning framework for short-term forecasting," *Environmental and Ecological Statistics*, p. 175182, 2021.
- [41] Thomas M. Cover, Joy A. Thomas, "Elements of Information Theory," *John Wiley and Sons*, 1991.
- [42] R. W. Yeung, *Strong Typicality - Information Theory and Network Coding*. Springer US, December 2008.
- [43] C. Chow and C. Liu, "Approximating discrete probability distributions with dependence trees," *IEEE Transactions on Information Theory*, vol. 14, no. 3, pp. 462–467, 1968.
- [44] D. Henderson, S. Jacobson, and A. Johnson, "The theory and practice of simulated annealing," *Handbook of Metaheuristics*, pp. 287–319, 04 2006.
- [45] Bengt Holter, "On the Capacity of the MIMO Channel - A Tutorial Introduction."
- [46] J. Choi, B. Evans, and A. Gatherer, "Resolution-adaptive hybrid mimo architectures for millimeter wave communications," *IEEE Transactions on Signal Processing*, vol. 65, no. 23, pp. 6201–6216, 2017.
- [47] Gilbert Strang, "Introduction to Linear Algebra," *Thomson, Fifth Edition*, 2005.
- [48] C. Pralet, T. Schiex, and G. Verfaillie, *Sequential Decision-Making Problems: Representation and Solution*. Wiley, 2009.
- [49] I. Z. Ahmed, H. R. Sadjadpour, and S. Yousefi, "Information-assisted dynamic programming for a class of constrained combinatorial problems," *IEEE Access*, vol. 10, pp. 87 816–87 831, 2022.
- [50] Y. Xu and W. Yin, "A globally convergent algorithm for nonconvex optimization based on block coordinate update," 2014. [Online]. Available: <https://arxiv.org/abs/1410.1386>

APPENDIX

A. Expression for CRLB

We have $\mathbf{K} = \alpha \mathbf{W}_S \Phi \mathbf{F}_S$, $\mathbf{K}^{-1} = \frac{1}{\alpha} \mathbf{F}_S^{-1} \Phi^{-1} \mathbf{W}_S^{-1}$,

$$(\mathbf{K}^H)^{-1} = \frac{1}{\alpha} (\mathbf{W}_S^H)^{-1} \Phi (\mathbf{F}_S^H)^{-1}, \quad (59)$$

$$\mathbf{C} = \alpha^2 \sigma_n^2 \mathbf{W} \mathbf{W}^H + \mathbf{W}_S \tilde{\mathbf{W}}_D^H \mathbf{D}_q^2 \tilde{\mathbf{W}}_D \mathbf{W}_S^H,$$

Substituting the terms in (59) for the CRLB expression, we have

$$\begin{aligned} \mathbf{I}^{-1}(\hat{\mathbf{x}}) &= (\mathbf{K}^H \mathbf{C}^{-1} \mathbf{K})^{-1} = \mathbf{K}^{-1} \mathbf{C} (\mathbf{K}^H)^{-1}, \\ &= \frac{1}{\alpha} \mathbf{F}_S^{-1} \Phi^{-1} \mathbf{W}_S^{-1} \left[\alpha^2 \sigma_n^2 \mathbf{W} \mathbf{W}^H \right] \frac{1}{\alpha} (\mathbf{W}_S^H)^{-1} \Phi (\mathbf{F}_S^H)^{-1} + \\ &\frac{1}{\alpha^2} \mathbf{F}_S^{-1} \Phi^{-1} \mathbf{W}_S^{-1} \left[\mathbf{W}_S \tilde{\mathbf{W}}_D^H \mathbf{D}_q^2 \tilde{\mathbf{W}}_D \mathbf{W}_S^H \right] (\mathbf{W}_S^H)^{-1} \Phi (\mathbf{F}_S^H)^{-1}, \\ &= \mathbf{F}_S^{-1} \left[\sigma_n^2 \Phi^{-1} \tilde{\mathbf{W}} \Phi + \frac{1}{\alpha^2} \Phi^{-1} \tilde{\mathbf{W}}_D^H \mathbf{D}_q^2 \tilde{\mathbf{W}}_D \Phi \right] (\mathbf{F}_S^H)^{-1}, \end{aligned}$$

where $\tilde{\mathbf{W}} = \tilde{\mathbf{W}}_D^H \mathbf{W}_A^H \mathbf{W}_A \tilde{\mathbf{W}}_D$.

(60)

B. Expression for the information rate and energy efficiency

Considering (23), we can write the expression for the information-rate of the MaMIMO channel as function of the RIS phase shift matrix Φ as [32]

$$\begin{aligned} R(\Phi) &= I(\mathbf{x}; \mathbf{y}) = h(\mathbf{y}) - h(\mathbf{y}|\mathbf{x}) \\ &= h(\mathbf{y}) - h(\mathbf{K}\mathbf{x} + \mathbf{n}_1|\mathbf{x}) \stackrel{(a)}{=} h(\mathbf{y}) - h(\mathbf{n}_1), \end{aligned} \quad (61)$$

where $I(\mathbf{x}; \mathbf{y})$ is the mutual information of random variables \mathbf{x} and \mathbf{y} , and \mathbf{K} is a function of the RIS phase shift matrix Φ . (a) holds if and only if both \mathbf{n}_q and \mathbf{x} are Gaussian. Hence, ensures \mathbf{y} is Gaussian. Also, if $\mathbf{y} \in \mathbb{C}^N$, then the differential entropy $h(\mathbf{y})$ is less than or equal to $\log_2 \det(\pi e \mathbf{B})$ with equality if and only if \mathbf{y} is circularly symmetric complex Gaussian with $E[\mathbf{y}\mathbf{y}^H] = \mathbf{B}$ [45]. That is

$$\begin{aligned} \mathbf{B} &= E[(\mathbf{K}\mathbf{x} + \mathbf{n}_1)(\mathbf{K}\mathbf{x} + \mathbf{n}_1)^H] \\ &= E[\mathbf{K}\mathbf{x}\mathbf{x}^H \mathbf{K}^H + \mathbf{n}_1 \mathbf{n}_1^H] = p \mathbf{K} \mathbf{K}^H + \mathbf{C}. \end{aligned} \quad (62)$$

where $\mathbf{C} = \alpha^2 \sigma_n^2 \mathbf{W} \mathbf{W}^H + \mathbf{W}_S \tilde{\mathbf{W}}_D^H \mathbf{D}_q^2 \tilde{\mathbf{W}}_D \mathbf{W}_S^H$. The differential entropies $h(\mathbf{y})$ and $h(\mathbf{n}_1)$ satisfy

$$\begin{aligned} h(\mathbf{y}) &\leq \log_2 \det(\pi e \mathbf{B}) = \log_2 \det \left(\pi e (p \mathbf{K} \mathbf{K}^H + \mathbf{C}) \right), \\ h(\mathbf{n}_1) &\leq \log_2 \det(\pi e \mathbf{C}), \end{aligned} \quad (63)$$

with equality iff \mathbf{y} and \mathbf{n}_1 possess circularly symmetric complex Gaussian statistics. However, using the Theorem-1 in [32], it is straightforward to see that $\mathbf{n}_1 \sim \mathcal{CN}(\mathbf{0}, \mathbf{C})$. Hence we have

$$h(\mathbf{n}_1) = \log_2 \det(\pi e \mathbf{C}). \quad (64)$$

Thus the expression for the information rate in (61) can be rewritten as

$$\begin{aligned} R(\Phi) &= h(\mathbf{y}) - h(\mathbf{n}_1) \stackrel{(b)}{=} \log_2 \det(\pi e \mathbf{B}) - \log_2 \det(\pi e \mathbf{C}) \\ &= \log_2 \det \left(p \mathbf{K} \mathbf{K}^H \mathbf{C}^{-1} + \mathbf{I}_N \right), \end{aligned} \quad (65)$$

where (b) follows from the assumption that the input symbol vector \mathbf{x} is circular symmetric Gaussian vector that could be modeled as $\mathbf{x} \sim \mathcal{CN}(\mathbf{0}, p \mathbf{I}_N)$ [30], [32], [46]. The information rate in (65) can be further simplified as [32]

$$\begin{aligned} R(\Phi) &= \log_2 \det \left(p \mathbf{K} \mathbf{K}^H \mathbf{C}^{-1} \mathbf{K} \mathbf{K}^{-1} + \mathbf{K} \mathbf{K}^{-1} \right), \\ &= \log_2 \det \left(p \mathbf{K} (\mathbf{K}^H \mathbf{C}^{-1} \mathbf{K} + \frac{1}{p} \mathbf{I}_N) \mathbf{K}^{-1} \right), \\ &= \log_2 \det(p \mathbf{K}) \det \left(\mathbf{K}^H \mathbf{C}^{-1} \mathbf{K} + \frac{1}{p} \mathbf{I}_N \right) \det(\mathbf{K}^{-1}), \\ &= \log_2 p^N \det \left(\mathbf{K}^H \mathbf{C}^{-1} \mathbf{K} + \frac{1}{p} \mathbf{I}_N \right), \\ &= N \log_2 p + \log_2 \det \left((\mathbf{I}^{-1}(\hat{\mathbf{x}}))^{-1} + \frac{1}{p} \mathbf{I}_N \right). \end{aligned} \quad (66)$$

Since the MSE $\mathbf{M}(\mathbf{x})$ achieves the CRLB by the design of the precoders and combiners as seen in (16), we can also write

the information-rate as follows

$$R(\Phi) = N \log_2 p + \log_2 \det \left((\mathbf{M}(\mathbf{x}))^{-1} + \frac{1}{p} \mathbf{I}_N \right). \quad (67)$$

Similarly, we can define the energy efficiency (EE) as a function of the RIS phase matrix Φ as

$$\begin{aligned} \eta_{EE}(\Phi) &= \frac{R(\Phi)}{p(b)} \text{ (bits/Hz/Joule)} \\ &= \frac{N \log_2 p + \log_2 \det \left((\mathbf{M}(\mathbf{x}))^{-1} + \frac{1}{p} \mathbf{I}_N \right)}{P_T + P_R + P_{RIS} + 2Ncf_s 2^b}, \end{aligned} \quad (68)$$

where where $p(b)$ is the total power consumed. Here P_T , P_R , and P_{RIS} are the power consumed at the transmitter, receiver, and RIS respectively. The net ADC power consumption is $2Ncf_s 2^b$, where b is the ADC bit resolution used in all the N RF paths, c is the power consumed per conversion step and f_s is the sampling rate in Hz [31].

From (67) and (68), it can be shown that maximizing the information rate (throughput) R or maximizing the energy efficiency η_{EE} for a given (designed) hybrid precoders and combiners is equivalent to minimizing the CRLB $\mathbf{I}^{-1}(\hat{\mathbf{x}})$. This is shown using the Lemma 2 below

Lemma 2.

$$\max_{\Phi} R(\Phi) \Leftrightarrow \max_{\Phi} \eta_{EE}(\Phi) \Leftrightarrow \min_{\Phi} \mathbf{I}^{-1}(\hat{\mathbf{x}}). \quad (69)$$

Proof. We can decompose the squared MSE matrix $\mathbf{M}(\mathbf{x})$ in (13) as $\mathbf{M}(\mathbf{x}) = \mathbf{B}\mathbf{A}\mathbf{B}^{-1}$, where $\mathbf{A} = \text{diag}(\lambda_1, \lambda_2, \dots, \lambda_N)$; such that $\{\lambda_i\}_{i=1}^N$ are the eigenvalues of $\mathbf{M}(\mathbf{x})$. It is easy to note that $\mathbf{M}(\mathbf{x})$ is always a positive semidefinite matrix, and hence the eigenvalues $\{\lambda_i\}_{i=1}^N$ are real and positive [47]. We can further write (13) as

$$\delta(\Phi) \triangleq \text{tr}(\mathbf{M}(\mathbf{x})) = \text{tr}(\mathbf{A}). \quad (70)$$

The MSE δ can be minimized when $\delta_{\min}(\Phi) = \min_{\Phi} \sum_{i=1}^{N_s} \lambda_i$. Hence the condition for (70) to be minimized is $\lambda_i \rightarrow 0, \forall i \in [1, N_s]$.

Now, to maximize $R(\Phi)$ in (67) we can write

$$R_{\max}(\Phi) = N \log_2 p + \max_{\Phi} \log_2 \det \left((\mathbf{M}(\mathbf{x}))^{-1} + \frac{1}{p} \mathbf{I}_N \right), \quad (71)$$

Since the term $N \log_2 p$ is not dependent on Φ , and we know that the function $\log_2(\cdot)$ is monotonically increasing, it suffices to maximize the expression (72) to attain $R_{\max}(\Phi)$

$$\Phi^{R_{\max}} = \arg\max_{\Phi} \left\{ \det \left((\mathbf{M}(\mathbf{x}))^{-1} + \frac{1}{p} \mathbf{I}_N \right) \right\}. \quad (72)$$

We can write

$$\begin{aligned} \det(\mathbf{B}\mathbf{A}^{-1}\mathbf{B}^{-1} + \frac{1}{p}\mathbf{I}_N) &= \det(\mathbf{B}[\mathbf{A}^{-1} + \frac{1}{p}\mathbf{I}_N]\mathbf{B}^{-1}), \\ &= \det(\mathbf{A}^{-1} + \frac{1}{p}\mathbf{I}_N) = \prod_{i=1}^N \left(\frac{1}{\lambda_i} + \frac{1}{p} \right) = \prod_{i=1}^N \left(\frac{p + \lambda_i}{\lambda_i} \right). \end{aligned} \quad (73)$$

This implies $\Phi^{R_{\max}} = \arg\max_{\Phi} \left\{ \prod_{i=1}^N \left(\frac{p + \lambda_i}{\lambda_i} \right) \right\}$. Since the

eigenvalues are real and positive, the maximization (72) is achieved for a given p , when $\prod_{i=1}^N \lambda_i \rightarrow 0$ or $\lambda_i \rightarrow 0, \forall i \in [1, N]$, which is similar to the condition that was required to minimize the MSE δ .

For energy efficiency $\eta_{EE}(\Phi)$, maximizing the numerator $R(\Phi)$ is sufficient condition to maximize the same because the denominator does not depend on the Φ and can be treated as constant. \square

C. The RIS phase optimization as an MDP

The problem (30) can be visualized as a stochastic-sequential-decision-making (SSDM) problem [48]. The solution Φ at a given time or for a channel realization can be thought of as sequence of decisions to be taken to decide the phase-shifts of the M reflecting elements considering a probabilistic model. The phase-shift value of the first element is selected based on the initial probabilities of the phase-shifts. The subsequent elements phase-shifts are arrived based on the previous elements phase-shift using the prior and conditional distributions. Here the solution Φ can be thought of as a sequence of random variables $\Phi = \{\Phi_1, \Phi_2, \dots, \Phi_M\}$, where the discrete random variable Φ_i has a probability mass function (PMF) $p(\Phi_i)$. Also, $p(\Phi_i|\Phi_j)$ represents the transition probabilities across the two reflection elements i and j . Let the distribution $q(\Phi_1, \dots, \Phi_M)$ denote a prior distribution of the optimal solution to (30). An estimate of $q(\Phi_1, \dots, \Phi_M)$ can be sampled from the solution space of (30) as described in Section V-B1. The sequence in which the phase-shifts are decided is shown as

$$\Phi_1 \longrightarrow \Phi_2 \longrightarrow \Phi_3 \longrightarrow \dots \longrightarrow \Phi_M. \quad (74)$$

A measure of information called Information-to-go (\mathcal{I}_g) was introduced in [38]. The term \mathcal{I}_g is associated with a sequence that specifies cumulated information processing cost or bandwidth required to quantify the future decisions and actions. The measure (\mathcal{I}_g) defines how many bits on average the system needs to specify the future states in an SSDP (or its informational regret) with respect to the prior. This is written as

$$\mathcal{I}_g^{\Phi^m} = \mathbb{E}_{p(\Phi_{m+1}, \dots, \Phi_M | \Phi^m)} \log \frac{p(\Phi_{m+1}, \dots, \Phi_M | \Phi^m)}{q(\Phi_{m+1}, \dots, \Phi_M)}, \quad (75)$$

where $p(\Phi_{m+1}, \Phi_{m+2}, \dots, \Phi_M | \Phi^m)$ is the conditional distribution of the future looking sequence given a sequence Φ^m , and the fixed prior $q(\Phi_{m+1}, \Phi_{m+2}, \dots, \Phi_M)$. The term Φ^m indicates the partially observed (decided) sequence $\{\Phi_1, \Phi_2, \dots, \Phi_m\}$ for some $m \leq M$.

However, the analysis with (75) is more complex and difficult, hence an approximation to Markovicity is considered [38]. In which case, we can rewrite (75) as

$$\mathcal{I}_g^{\Phi^m} = \mathbb{E}_{p(\Phi_{m+1}, \dots, \Phi_M | \Phi_m)} \log \frac{p(\Phi_{m+1}, \dots, \Phi_M | \Phi_m)}{q(\Phi_{m+1}, \dots, \Phi_M)}. \quad (76)$$

In [38], the authors claim that "...the Markovicity condition seems, at first sight, a comparatively strong assumption which might seem to limit the applicability of the formalism for

modeling the subjective knowledge of an agent. However, under the knowledge of the full state, in the model the agent itself is not assumed to have full access to the state.” (Section 8.2 in [38]).

In the case when the prior $q(\Phi_{m+1}, \dots, \Phi_M)$ can also be sampled as conditionals, that is $q(\Phi_{m+1}, \dots, \Phi_M | \Phi_m)$, then we can rewrite (76) as

$$\mathcal{I}_g^{\Phi^m} = \mathbb{E}_{p(\Phi_{m+1}, \dots, \Phi_M | \Phi_m)} \log \frac{p(\Phi_{m+1}, \dots, \Phi_M | \Phi_m)}{q(\Phi_{m+1}, \dots, \Phi_M | \Phi_m)}. \quad (77)$$

Using chain rule and Markovicity, we can establish a recursive relationship for (77) [49]

$$\begin{aligned} \mathcal{I}_g^{\Phi^m} &= \mathbb{E}_{p(\Phi_{m+1}, \dots, \Phi_M | \Phi_m)} \log \frac{p(\Phi_{m+1}, \dots, \Phi_M | \Phi_m)}{q(\Phi_{m+1}, \dots, \Phi_M | \Phi_m)}, \\ &= \mathbb{E}_{p(\Phi_{m+1}, \dots, \Phi_M | \Phi_m)} \log \frac{p(\Phi_{m+1} | \Phi_m) \cdots p(\Phi_M | \Phi_{M-1})}{q(\Phi_{m+1} | \Phi_m) \cdots q(\Phi_M | \Phi_{M-1})}, \\ &= \mathbb{E}_{p(\Phi_{m+1} | \Phi_m)} \log \left[\frac{p(\Phi_{m+1} | \Phi_m)}{q(\Phi_{m+1} | \Phi_m)} \right] + \mathcal{I}_g^{\Phi^{m+1}}. \end{aligned} \quad (78)$$

Hence $\mathcal{I}_g^{\Phi^m}$ can be written as a value function with a recursive relationship that satisfy the Bellman’s optimality criterion [38], [49] and is a classical example of a MDP. It is also worth noting that effectively (78) can be written as

$$\mathcal{I}_g^{\Phi} = D_{KL}(p(\Phi_1, \dots, \Phi_M) || q(\Phi_1, \dots, \Phi_M)). \quad (79)$$

Intuitively, $\mathcal{I}_g^{\Phi} \approx 0$ implies that the least information is required to pursue the path Φ for optimality or near-optimality. On the other hand, a large value of \mathcal{I}_g^{Φ} implies considerable information is required to make the decision (or inability to make a decision) in pursuing the path Φ for optimality.

D. Alternating optimization

The problem in (80) can also be solved by updating just one or a few blocks of optimization variables ($\mathbf{F}_S, \mathbf{F}_A, \tilde{\mathbf{F}}_D, \Phi, \mathbf{W}_A^H, \tilde{\mathbf{W}}_D^H, \mathbf{W}_S$) using alternating optimization [24], [50].

$$\delta = \min_{\substack{\mathbf{F}_S, \mathbf{F}_A, \tilde{\mathbf{F}}_D, \Phi \\ \mathbf{W}_A^H, \tilde{\mathbf{W}}_D^H, \mathbf{W}_S}} \mathcal{L}(\mathbf{F}_S, \mathbf{F}_A, \tilde{\mathbf{F}}_D, \Phi, \mathbf{W}_A^H, \tilde{\mathbf{W}}_D^H, \mathbf{W}_S), \quad (80)$$

where $\mathcal{L}(\mathbf{F}_S, \mathbf{F}_A, \tilde{\mathbf{F}}_D, \Phi, \mathbf{W}_A^H, \tilde{\mathbf{W}}_D^H, \mathbf{W}_S) = \text{tr}(\mathbf{M}(\mathbf{x}))$. The algorithm is described below

Algorithm 3 Alternating optimization

```

1: procedure AO( $\mathbf{F}_S^0, \mathbf{F}_A^0, \tilde{\mathbf{F}}_D^0, \Phi^0, \mathbf{W}_A^{H0}, \tilde{\mathbf{W}}_D^{H0}, \mathbf{W}_S^0, \epsilon_T$ )
2:    $k \leftarrow 0$ 
3:    $\delta_k \leftarrow \mathcal{L}(\mathbf{F}_S^k, \mathbf{F}_A^k, \tilde{\mathbf{F}}_D^k, \Phi^k, \mathbf{W}_A^{Hk}, \tilde{\mathbf{W}}_D^{Hk}, \mathbf{W}_S^k)$ 
4:   do
5:     Solve for  $\mathbf{F}_A, \tilde{\mathbf{F}}_D$  using MSER-Precoding in [24]
6:      $\{\mathbf{F}_A^{k+1}, \tilde{\mathbf{F}}_D^{k+1}\} \leftarrow$ 
7:      $\text{argmin}_{\mathbf{F}_A, \tilde{\mathbf{F}}_D} \mathcal{L}(\mathbf{F}_S^k, \mathbf{F}_A, \tilde{\mathbf{F}}_D, \Phi^k, \mathbf{W}_A^{Hk}, \tilde{\mathbf{W}}_D^{Hk}, \mathbf{W}_S^k)$ 
8:     Solve for  $\mathbf{W}_A^H, \tilde{\mathbf{W}}_D^H$  using (22)
9:      $\{\mathbf{W}_A^{Hk+1}, \tilde{\mathbf{W}}_D^{Hk+1}\} \leftarrow$ 
10:     $\text{argmin}_{\mathbf{W}_A^H, \tilde{\mathbf{W}}_D^H} \mathcal{L}(\mathbf{F}_S^k, \mathbf{F}_A^{k+1}, \tilde{\mathbf{F}}_D^{k+1}, \Phi^k, \mathbf{W}_A^H, \tilde{\mathbf{W}}_D^H, \mathbf{W}_S^k)$ 

```

```

11:   Solve for  $\Phi$  using eMSER-Reflecting in [24]
12:    $\Phi^{k+1} \leftarrow$ 
13:    $\text{argmin}_{\Phi} \mathcal{L}(\mathbf{F}_S^k, \mathbf{F}_A^{k+1}, \tilde{\mathbf{F}}_D^{k+1}, \Phi, \mathbf{W}_A^{Hk+1}, \tilde{\mathbf{W}}_D^{Hk+1}, \mathbf{W}_S^k)$ 
14:   Solve for  $\mathbf{F}_S, \mathbf{W}_S$  using (31) and (32)
15:    $\{\mathbf{F}_S^{k+1}, \mathbf{W}_S^{k+1}\} \leftarrow \text{argmin}_{\mathbf{F}_S, \mathbf{W}_S} \mathcal{L}(\mathbf{F}_S, \mathbf{F}_A^{k+1}, \tilde{\mathbf{F}}_D^{k+1}, \Phi^{k+1},$ 
16:      $\mathbf{W}_A^{Hk+1}, \tilde{\mathbf{W}}_D^{Hk+1}, \mathbf{W}_S)$ 
17:    $\delta_{k+1} \leftarrow$ 
18:    $\mathcal{L}(\mathbf{F}_S^{k+1}, \mathbf{F}_A^{k+1}, \tilde{\mathbf{F}}_D^{k+1}, \Phi^{k+1}, \mathbf{W}_A^{Hk+1}, \tilde{\mathbf{W}}_D^{Hk+1}, \mathbf{W}_S^{k+1})$ 
19:    $err \leftarrow \delta_k - \delta_{k+1}$ 
20:    $k \leftarrow k + 1$ 
21:   while  $\{err > \epsilon_T\}$ 
22: end procedure

```



I. Zakir Ahmed (Member, IEEE) received his Bachelors degree in Electrical Engineering from UVCE, Bengaluru, and an M.S. degree from Illinois Institute of Technology, Chicago. He is currently pursuing his Ph.D. Degree in Electrical Engineering from the University of California at Santa Cruz. He has over 20 years of industry experience as a researcher, design engineer, and practitioner in wireless communication and signal processing domains. He worked in the Motorola DSP group in Bangalore, India, from 2000 to 2009. He worked as an RF engineer with National Instruments from 2009 to 2020. Since 2020 he has been based out of San Diego, California, working as a Machine-learning research engineer for applications in RF systems. He holds more than ten US patents and has several research publications in the areas of wireless communication and signal processing. His research interests include optimization methods, signal processing, wireless communication, information theory, and machine learning.



Hamid R. Sadjadpour (Senior Member, IEEE) received the B.S. and M.S. degrees from Sharif University of Technology, and the Ph.D. degree from University of Southern California (USC). In 1995, he joined the AT&T Shannon Research Laboratory, as a Technical Staff Member and later as a Principal Member of Technical Staff. In 2001, he joined the University of California at Santa Cruz where he is currently a Professor. He has authored over 200 publications and holds 20 patents. His research interests are in the general areas of wireless communications, security and networks. He has served as a Technical Program Committee Member and the Chair in numerous conferences. He is a co-recipient of the best paper awards at the 2007 International Symposium on Performance Evaluation of Computer and Telecommunication Systems, the 2008 Military Communications conference, the 2010 European Wireless Conference, and the 2017 Conference on Cloud and Big Data Computing.



Shahram Yousefi (Senior Member, IEEE) has 25 years of experience in engineering, technology, teaching, managing teams and projects, as well as public speaking and advising. He received his B.Sc. in electrical engineering from University of Tehran and his PhD in telecom from the University of Waterloo in Canada. He has been with the University of Toronto, Canada, Ecole Polytechnique Fdral de Lausanne (EPFL), Switzerland, Jilin University, China, University of California, Santa Cruz, USA, and Queen’s University, Kingston, Canada, where

he is currently a tenured full professor and Associate Dean of Corporate Relations. Shahram has served as the Editor-in-Chief of the IEEE CJECE journal and has received more than 20 awards and scholarships including the Golden Apple teaching award as well as the Natural Sciences and Engineering Research Council of Canada’s Discovery Accelerator Supplement (NSERC DAS) award. His research interests include communications, cloud systems, big data, networks, information theory, signal processing, control, algorithms, and machine intelligence in which he holds a number of patents. He co-founded Canarmony Corp. (2014), MESH Scheduling Inc. (2018), and OPTT Inc. (2018) to apply algorithms to make life better and more harmonious. One of Shahram’s patents in the area of data storage was licensed to revolutionize a \$500b solid state storage industry. Shahram admires entrepreneurs and advises a number of ventures.